Article

SARS-CoV-2-specific plasma cells are not durably established in the bone marrow long-lived compartment after mRNA vaccination

Check for updates

Doan C. Nguyen [1], Ian T. Hentenaar[1], Andrea Morrison-Porter[1], David Solano[1], Natalie S. Haddad [1], Carlos Castrillon[2], Martin C. Runnstrom[1,5], Pedro A. Lamothe [1], Joel Andrews[3], Danielle Roberts[3], Sagar Lonial[3], Ignacio Sanz [2,4] & F. Eun-Hyung Lee [1,4] ✉

Severe acute respiratory syndrome coronavirus 2 (SARS-CoV-2) mRNA vaccines are effective at protecting from severe disease, but the protective antibodies wane rapidly even though SARS-CoV-2-specific plasma cells can be found in the bone marrow (BM). Here, to explore this paradox, we enrolled 19 healthy adults at 2.5–33 months after receipt of a SARS-CoV-2 mRNA vaccine and measured influenza-, tetanus- or SARS-CoV-2-specific antibody-secreting cells (ASCs) in long-lived plasma cell (LLPC) and non-LLPC subsets within the BM. Only influenza- and tetanus-specific ASCs were readily detected in the LLPCs, whereas SARS-CoV-2 specificities were mostly absent. The ratios of non-LLPC:LLPC for influenza, tetanus and SARS-CoV-2 were 0.61, 0.44 and 29.07, respectively. In five patients with known PCR-proven history of recent infection and vaccination, SARS-CoV-2-specific ASCs were mostly absent from the LLPCs. We show similar results with measurement for secreted antibodies from BM ASC culture supernatant. While serum IgG titers specific for influenza and tetanus correlated with IgG LLPCs, serum IgG levels for SARS-CoV-2, which waned within 3–6 months after vaccination, were associated with IgG non-LLPCs. In all, our studies suggest that rapid waning of SARS-CoV-2-specific serum antibodies could be accounted for by the absence of BM LLPCs after these mRNA vaccines.

As of August 2024, severe acute respiratory syndrome coronavirus 2 (SARS-CoV-2) has infected over 776 million people worldwide and killed 7.1 million, including 1.2 million in the United States alone[1]. While the original wild-type SARS-CoV-2 primary vaccine series and boosters have been effective against severe disease, hospitalization and death, protection by sterilizing immunity against infection or transmission has not been demonstrated. SARS-CoV-2 vaccines appear to provide lasting T cell responses; however, waning neutralizing antibody levels within 3–6 months result in breakthrough infection or reinfections with the same strain[2–4]. Therefore, we asked whether subjects after SARS-CoV-2 vaccination develop spike specificity in the long-lived plasma cell (LLPC) subset (CD19−CD38hiCD138+) of the human bone marrow (BM)[5]. For clarity, the term ASC refers to all antibody-secreting cells (ASCs), which include early-minted ASCs (oftentimes referred to as plasmablasts[6]) and more mature ASCs known as plasma cells that can contain LLPCs.

Early in the coronavirus disease 2019 (COVID-19) pandemic, studies reported that SARS-CoV-2 spike IgG ASCs were readily identified in the BM after SARS-CoV-2 infection[7] or messenger RNA vaccination[8], and in nonhuman primates after SARS-CoV-2 spike protein vaccination[9], suggesting long-lived humoral protection without evidence of longitudinal serologic data. Interestingly, BM ASC compartments can be quite diverse, comprising of LLPCs as well as early-minted ASCs (new arrivals) of which many may die, while some progressively mature into LLPCs[10–15]. How LLPCs are generated is not entirely clear, but after vaccination, the majority of ASCs released from secondary lymph nodes are destined to undergo apoptosis unless they finally arrive in the specialized BM survival niches filled with mesenchymal stromal cells and myeloid cells. This niche provides important factors for ASC survival and maturation such as IL-6 and APRIL[16,17]. These new arrivals can further differentiate into a mature long-lived phenotype (CD19−CD138+), which secretes neutralizing antibodies for decades[10,11]. Although the human BM is a reservoir of LLPCs, new arrivals, including CD19+CD138− and intermediate phenotypes of CD19+CD138+ ASCs, make it quite heterogeneous[12,18], such that mere presence to this locale may not reflect durability.

Tetanus vaccination generates antigen-specific BM LLPCs and affords safeguards for decades with a serologic half-life of 10 years[10,19]. For influenza, humoral immune protection provided by influenza vaccines typically wanes within 4–6 months[20]. Infants may have pre-existing maternally derived anti-influenza antibodies although they wane over the first 6 months of life[21]. Unvaccinated individuals are estimated to have their first influenza infection within 5 years of birth[22] and to be infected with a new influenza virus strain every 3–7 years[23]. Furthermore, newly induced immune responses are enhanced owing to cross-reactive antibodies from infections and reinfections with antigenically similar influenza virus strains[24–28]. Importantly, natural influenza infection generates long-lasting humoral immunity to the infecting strain, as shown in elderly adults who maintained neutralizing antibodies to the 1918 Spanish influenza virus nearly 90 years after the primary infection[29].

Here, we measure SARS-CoV-2 spike-specific ASCs in multiple BM compartments up to 33 months after SARS-CoV-2 mRNA vaccination and compare them with well-known long-lived responses such as tetanus- and influenza-specific ASCs and show the absence of SARS-CoV-2-specific ASCs in the BM LLPCs. This finding provides a mechanistic explanation for the short duration of systemic antibody responses to SARS-CoV-2 mRNA vaccines.

Results

Demographic and clinical characteristics

From May 2021 until March 2024, we enrolled 19 healthy adults aged of 20–65 years old (Fig. 1a). The subjects were recruited for BM aspirates 2.5–33 months after receiving the first dose of SARS-CoV-2 mRNA vaccines. All received a total of two to five vaccine doses, and BM aspirates were obtained 0.5–21 months after receiving the last booster (the third, fourth or fifth dose) (Table 1). One subject provided three longitudinal BM samples over a period of 21 months and a second subject had two aspirates over 6 months, resulting in a total of 22 BM aspirates. Five subjects reported infection with SARS-CoV-2 1–16 months before the BM collection, of which three subjects had infection once and two had two PCR-proven SARS-CoV-2 infections. These infections occurred 1–15.5 months after receiving the most recent vaccine dose. All 19 individuals received the quadrivalent influenza vaccine within 1–12 months (relative to the time of each BM aspirate), and one was delayed for 1 year due to the COVID-19 pandemic. All received the childhood series of the tetanus toxoid vaccine with recent boosters ranging from 1 month to 24 years from the time of BM aspirates.

BM ASC subsets and antigen optimization

BM ASC subsets were fluorescence-activated cell sorting (FACS)-sorted according to surface expression of CD19, CD38 and CD138[10] (Fig. 1b).

To overcome the problem with the rapid death of ASCs ex vivo[16], we rested the ASCs overnight in a new human in vitro plasma cell survival system that is capable of maintaining human ASC viability for months[16]. Since we had previously localized the BM LLPC compartment into PopD (CD19−CD38hiCD138+)[10], this population was sorted out of total BM ASCs together with non-LLPC subsets: PopA (CD19+CD38hiCD138−) and PopB (CD19+CD38hiCD138+). All were tested for total IgG secretion as well as influenza (Flu)-, tetanus toxoid (Tet)- and SARS-CoV-2-specific IgG secretion by bulk ELISpots. To optimize antigen detection for the BM ASC ELISpot assays, we collected early-minted blood ASCs (CD27hiCD38hi; Extended Data Fig. 1) 6–7 days after Flu, Tet or SARS-CoV-2 vaccination, which is the peak time for enrichment of vaccine-specific ASCs in the blood after secondary immunization[30,31], and performed ELISpots (Extended Data Fig. 2a). Of the SARS-CoV-2 antigens (S1 domain of spike protein (S1), S2 domain of spike protein (S2), receptor-binding domain (RBD), S-2P variant of spike protein (S2P), N-terminal domain (NTD) and nucleocapsid protein (NP)), S2P, a prefusion-stabilized spike trimer[32], generated the highest frequency, followed by S1 (with no significant difference; $P = 0.21$) (Fig. 1c,d), and so S2P was selected for the BM ASC ELISpot assays. We also validated the quadrivalent Flu vaccine (seasons of 2019–2020 to 2023–2024) as the Flu antigen and Tet antigen (Extended Data Fig. 2b,c), using blood ASCs at days 6–7, the peak of the respective ASC vaccine responses[30,31].

Absence of SARS-CoV-2-specific IgG BM LLPCs

Since BM aspirates can yield variable cell numbers, we included BM aspirates with >3,000 sorted cells in each of the three ASC populations, cultured the cells overnight in a specialized in vitro BM mimetic system[16] and performed bulk ELISpots (Fig. 2a; see also Methods). Among the BM subjects, sufficient cells to confidently measure vaccine specificities within PopA, PopB and PopD were obtained from 8, 15 and 17 individuals. As previously shown, all BM ASC subsets had detectable total IgG ASCs. Similar to previous reports[10], PopD contained the highest percentage of Flu and Tet IgG ASCs per total IgG ASCs: mean 7.3% (7.31 ± 3.51) and 2.1% (2.14 ± 1.70), respectively (Fig. 2b,c). PopB was readily populated with Flu and Tet IgG ASCs: mean 3.4% (3.43 ± 1.68) and 0.8% (0.77 ± 0.87), respectively, while PopA had the lowest frequencies: mean 1% (1.0 ± 0.66) and 0.2% (0.17 ± 0.17), respectively. Strikingly, within the same subjects, we could rarely detect S2P ASCs in PopD: mean 0.1% (0.14 ± 0.23). In contrast, the S2P specificity was readily found in PopB and PopA at frequencies comparable to Tet and Flu: mean 3.1% (3.13 ± 2.82) and 0.9% (0.89 ± 1.3), respectively.

Although the frequencies of Tet IgG ASC in PopA versus PopB showed no statistically significant difference, the frequencies of Flu IgG were higher in PopB over PopA. For both Flu and Tet IgG ASC, the frequencies in PopD were always higher than in PopB. In contrast, the S2P IgG ASC frequencies were always significantly lower in PopD compared with PopB (Fig. 2b,c). On average, the fold changes of IgG ASC specificities within PopD were 52.8 for Flu:S2P and 15.5 for Tet:S2P (Supplementary Table 1). In comparison, the fold changes of IgG ASC specificities within PopB were 1.1 for Flu:S2P and 0.3 for Tet:S2P. For S2P specificity, the fold changes of PopA:PopD was 6.4 and of PopB:PopD was 22.6 (Supplementary Table 2). In comparison, for Flu or Tet specificities, these fold changes were ≤0.47. Overall, the ratios of non-LLPC:LLPC for Flu, Tet and S2P were 0.61, 0.44 and 29.07, respectively (Fig. 2d). Thus, S2P IgG ASC are largely excluded from PopD.

Absence of SARS-CoV-2-specific IgA BM LLPC

Similar to IgG ASC, the frequencies of Flu and Tet IgA ASC were highest in PopD with a mean of 1.7% (1.70 ± 0.45) and 0.3% (0.31 ± 0.12), respectively, while frequencies in PopA and PopB were lower: for Flu, mean 0.8% (0.82 ± 0.43) and 1.4% (1.35 ± 1.32), respectively, and for Tet, 0.2% (0.24 ± 0.34) and 0.1% (0.11 ± 0.10), respectively (Extended Data Fig. 3a,b). Consistent with previous studies[33], these results may be explained by the predominance of IgG responses to the intramuscular
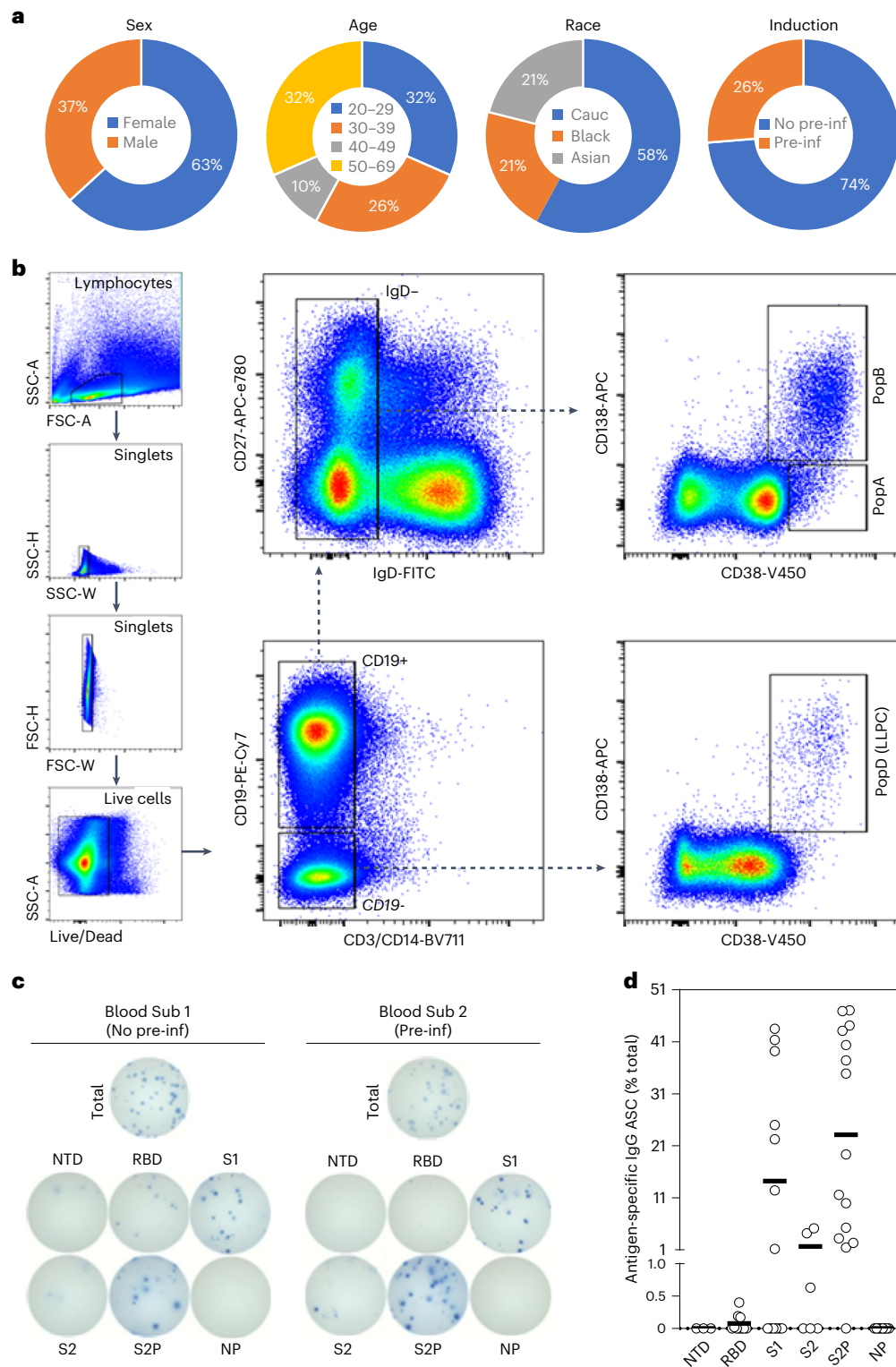
Fig. 1 | Demographics of the 19 BM subject cohort. a, The general FACS gating strategy used for sorting BM ASC subsets. Age given in years. Cauc, Caucasian; Pre-inf, previous (COVID-19) infection. **b**, BMMCs were first gated for lymphocytes, singlets and viable cells (based on their forward scatter/side scatter (FSC/SSC) and live/death properties). CD3 and CD14 were then used as dump markers to capture CD19+ and CD19− B cell populations. Subsequent subgating from CD19+ population on the IgD− fraction (versus CD27) and using CD138 versus CD38 allowed the breakdown of BM ASC populations into three subsets of interest: PopA (CD19+CD38hiCD138−), PopB (CD19+CD38hiCD138+) and PopD (LLPC; CD19−CD38hiCD138+). PE-Cy7, PE-Cyanine7 tandem fluorophore. **c**, Representative ELISpot scanned images (left: a vaccinated subject without previous COVID-19 infection; right: a vaccinated subject with previous COVID-19

infection). The numbers of input ASC that were incubated for total IgG: ~687 (left) or ~522 (right), and for antigen-specific ASC IgG: ~2,062 (left) or ~1,566 (right). Each circle represents an individual vaccine subject. The counts were provided by the sorters. Blood ASCs from subjects were collected at the peak time of response (which is 5–7 days post-vaccine). **d**, Frequencies (%) of antigen-specific IgG ASCs per total IgG ASCs. Data were generated from 3, 10, 13, 6, 15 and 8 different SARS-CoV-2-vaccinated subjects for SARS-CoV-2 antigens NTD, RBD, S1, S2, S2P and NP, respectively. Statistics were assessed using Student's *t*-test (two-tailed unpaired *t*-test) in Excel (Microsoft), and differences were considered significant at *P* values less than 0.05. For additional antigen selection and validation, see Extended Data Fig. 2. In **c** and **d**, it can be seen that S2P was most sensitive to capture SARS-CoV-2-specific blood ASCs isolated after SARS-CoV-2 mRNA vaccines.

Table 1 | BM subjects and BM samples

Year and subject ID	2020 (Tet/Flu history)	2021	2022	2023	2024	Pfizer	Moderna	Age	Sex	Race
Sub1	Tet (08/2018); Flu; Inf	V1; V2;Inf; BM	*V3*		*V4*	✓		31	F	Caucasian
Sub2	Tet (05/2017); Flu	V1 V2; BM; V3; V4				✓		26	M	Caucasian
Sub3	Tet (11/2011); Flu	V1 V2; BM; *Flu*; *V3*					✓	22	F	Caucasian
Sub4 (2021)	Tet (pre-2013); Flu	V1 V2; BM; V3; Inf	*V4*; *V5; Flu*	*Tet*		✓	✓	56	F	Asian
Sub5	Tet (pre-2008); Flu	V1 V2; Tet; BM Flu; V3					✓	23	F	Asian
Sub6	Tet (pre-2011); Flu	V1 V2; Flu BM	*V3*; *V4*; *V5*			✓		56	F	Asian
Sub7	Tet (06/2013)	Inf; V1 V2; Flu; V3; BM; *Inf*				✓		26	F	Caucasian
Sub8	Tet (pre-2011); Flu	V1 V2; Tet V3 Flu; *Flu*	BM; *Flu*				✓	42	M	Caucasian
Sub9 (2022)	Tet (pre-2010); Tet; Flu	V1 V2; Flu	V4 BM; *Flu*				✓	55	F	Caucasian
Sub10	Tet (pre-2011); Flu	V1; V2; Tet; Flu; V3	BM; *V4*				✓	36	M	Caucasian
Sub11	Tet (pre-2012); Flu	V1 V2; V3; Flu	V4; BM			✓		20	F	Black
Sub12	Tet (pre-2010); Tet; Flu	V1 V2; V3 Flu; Inf	V4; Flu; V5; BM				✓	63	F	Black
Sub13	Tet (pre-2010); Tet Flu	V1; Flu; V2	Flu; V4; BM			✓		48	M	Caucasian
Sub14	Tet (pre-2010); Flu (pre-2020)	V1 V2 BM	BM	*BM*			✓	63	M	Black
Sub15 (2023)	Tet (05/1999); Flu	V1; V2; Flu	V3; Flu	BM		✓		36	M	Caucasian
Sub16	Tet (09/2017); Flu	V1 V2; Flu; Inf	Inf; V3; Flu	BM		✓		65	F	Black
Sub17	Tet (pre-2012); Flu	V1 V2; Flu; V3	Inf; *Tet; Flu*	*BM*		✓		30	F	Caucasian
Sub18	Tet (07/2009); Flu	V1; V2; Flu	*Flu* V3	*Flu* *BM*		✓		28	F	Asian
Sub19	Tet (06/2015); Flu	V1; Flu	Flu V2	Flu BM	*BM*	✓	✓	30	M	Caucasian

Inf, infected with SARS-CoV-2; Sub, subject; Tet, tetanus vaccination; Flu, influenza vaccination; V1–V5, dose 1–5 of SARS-CoV-2 vaccine; F, female; M, male. Italics indicatete occurrence after BM aspirate. For multiple-aspirate subjects, age at the most recent BM aspirate is given.
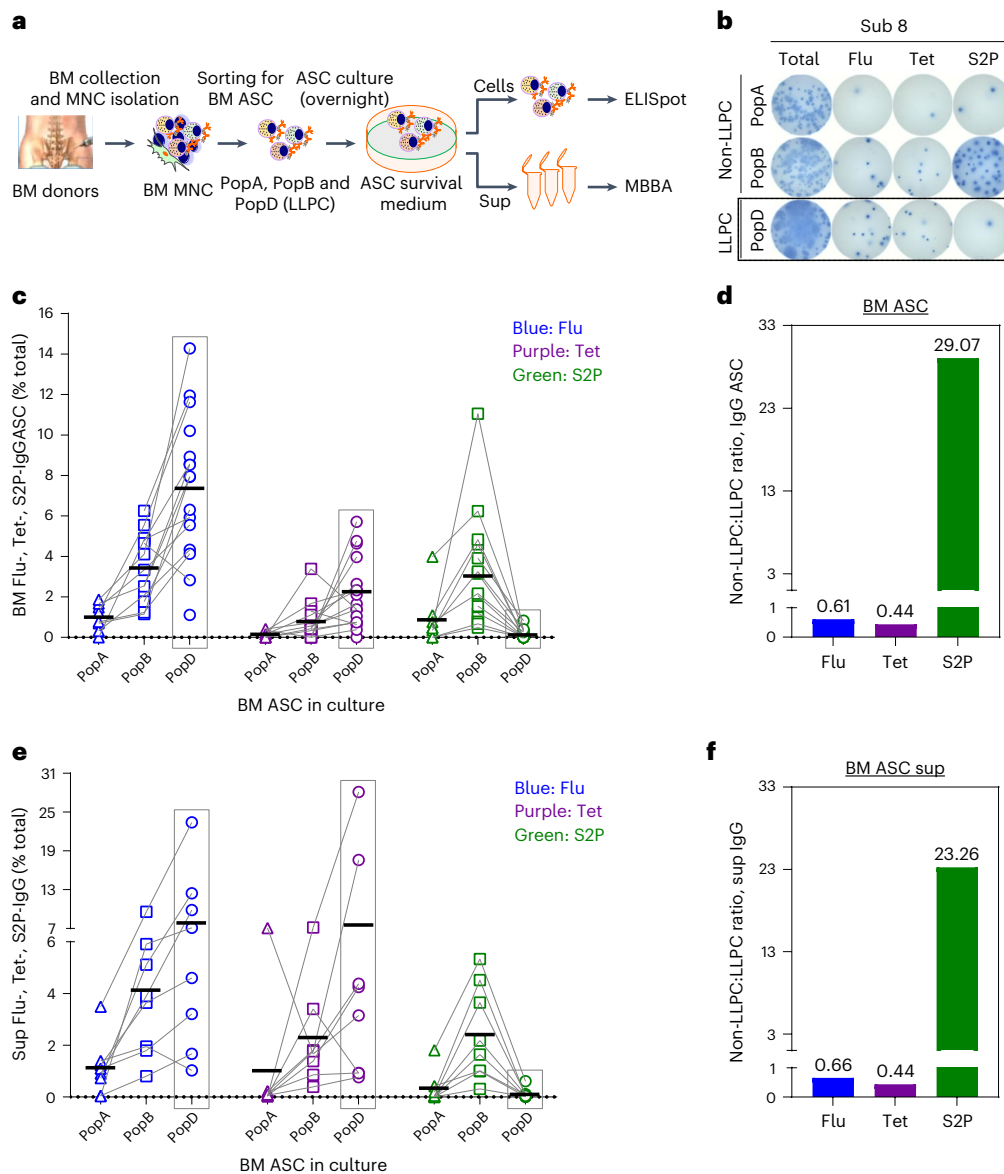
Fig. 2 | Absence of SARS-CoV-2 BM IgG LLPC after SARS-CoV-2 mRNA vaccines by detection of ASC and secreted IgG in the BM ASC culture supernatants.
**a**, Summary of the techniques and the experimental designs for detection of total, Flu, Tet and S2P ASCs and secreted IgG by ELISpots and MBBA, respectively. MNC, mononuclear cells. **b**, Representative ELISpot scanned images. The numbers of input ASC that were incubated were ~52 K, ~12.1 K and ~10.1 K for PopA, PopB and PopD, respectively. Each symbol represents an individual vaccine subject for total IgG and antigen-specific ASC from PopA, PopB and PopD. **c**, ELISpots measuring BM IgG ASC specific for Flu, Tet and S2P. Data were generated from 8, 15 and 17 different SARS-CoV-2-vaccinated subjects for PopA, PopB and PopD, respectively. For individual ratios and statistic comparisons between any two antigens for any subset or between any two subsets for any antigen, see Supplementary Tables 1 and 2, respectively. **d**, Fold difference (ratios) when comparing different vaccine specificities between non-LLPCs

(combined PopA and PopB) versus LLPCs (PopD). **e**, MBBA measuring IgG specific for Flu, Tet and S2P (normalized to total IgG) from culture supernatant of PopA, PopB and PopD. Supernatant preps were collected from 18–24-h cultures of BM ASCs after revival from the FACS sorters and were quantified for total IgG and vaccine-specific IgG in neat (undiluted). Data were generated from eight different SARS-CoV-2-vaccinated subjects. For individual ratios and statistic comparisons between any two antigens for any subset or between any two subsets for any antigen, see Supplementary Tables 1 and 2, respectively. **f**, The fold difference (ratios) when comparing normalized vaccine-specific IgG in the supernatants from the culture of non-LLPCs (combined PopA and PopB) versus LLPCs (PopD). For ratio calculation, see Methods. For IgG standard versus MFI curve, see Extended Data Fig. 4. Counts were provided by the sorters. LLPC, boxes in **b**, **c**, and **e**. Sub, subject; Sups, BM ASC culture supernatant preps. For details of subjects and samples, see Table 1.

tetanus vaccine. S2P IgA ASCs were also detected predominantly in PopA and PopB: a mean of 1.5% (1.46 ± 1.57) and 0.9% (0.90 ± 0.66), respectively, and were virtually absent in PopD: a mean of 0.03% (0.03 ± 0.06) (Extended Data Fig. 3b). On average, the fold changes of IgA ASC specificities within PopD were 50.9 for Flu:S2P and 9.3 for Tet:S2P (Supplementary Table 3). For S2P specificity, the fold change of PopA:PopD was 43.8 and of PopB:PopD was 27.0 (Supplementary Table 4). Thus, similar to IgG ASCs, other class-switched isotypes such as S2P IgA ASC are also mostly excluded from PopD (albeit small sample size).

Absence of SARS-CoV-2-specific IgG in LLPC culture supernatant

To validate the antigen-specific ELISpot results, we measured secreted IgG from BM ASC subsets (Fig. 2a; see also Methods). Briefly, from eight individuals who yielded sufficient sorted cells for all BM ASC subsets (PopA, PopB and PopD), we cultured ASCs in a specialized in vitro BM mimetic system overnight[16] and measured the cultured supernatants for secreted IgG specific for Flu, Tet and S2P by multiplex bead-binding assays (MBBAs)[34] (Extended Data Fig. 4). The results were similar to the
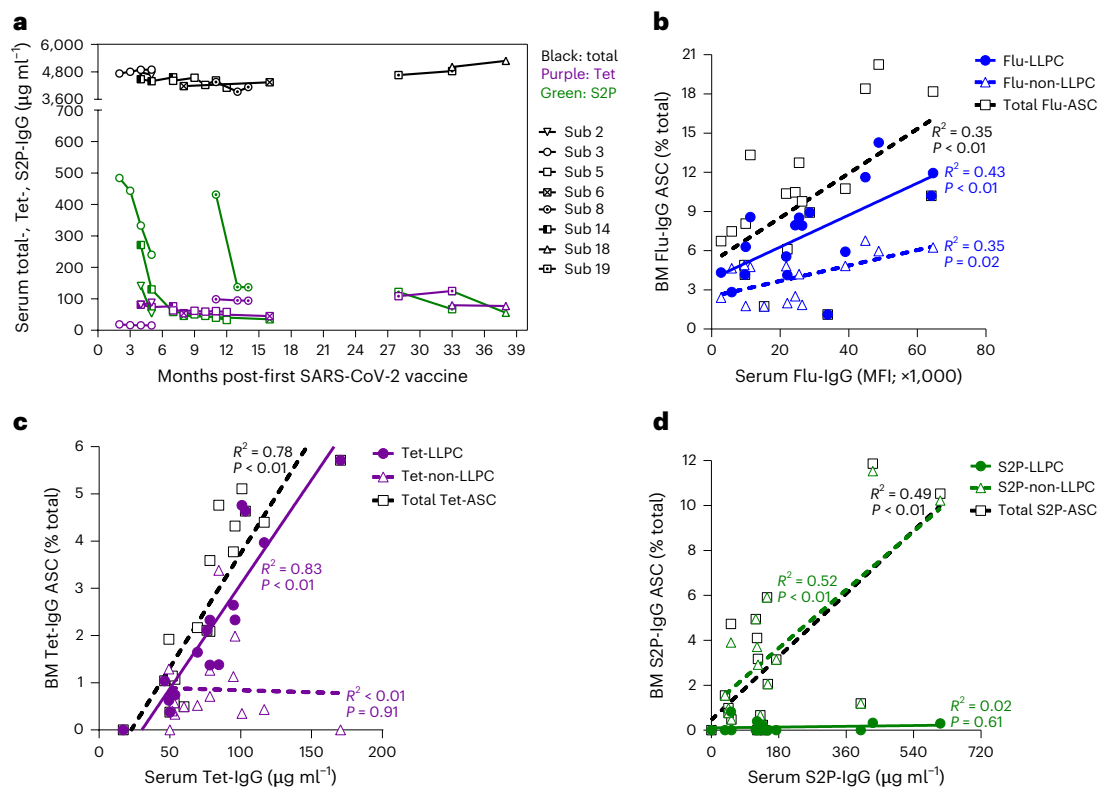
Fig. 3 | Vaccine-specific IgG levels in the serum: kinetics and magnitude, and correlation with BM IgG ASC responses. a, Kinetics and magnitude of IgG titers from subjects ($n = 8$) with at least two sequential serum samples (collected before the additional SARS-CoV-2 vaccines). **b–d**, Serum IgG levels versus BM IgG LLPC, non-LLPC and total ASC responses for Flu (**b**), Tet (**c**) and S2P (**d**) specificities in all examined subjects ($n = 19$). Sera collected within 5 months of the time of BM aspiration. For **b–d**, data were generated from eight different SARS-CoV-2-vaccinated subjects and correlations were assessed using simple linear regression analysis performed with GraphPad Prism (GraphPad Software). The exact P values for vaccine-specific LLPCs, non-LLPCs and total ASCs are 0.0043, 0.0196 and 0.0075, respectively (**b**); <0.0001, 0.91 and <0.0001, respectively (**c**); and 0.6096, 0.0025 and 0.0008, respectively (**d**). All serum samples tested at dilutions of 1:1,000–1:100,000 (total IgG) or 1:200–1:16,000 (antigen-specific IgG). For serum total and vaccine-specific IgG standard curves, see Supplementary Fig. 1. For details of subjects and samples, see Table 1.

ELISpot: the percentages of Flu and Tet IgG per total IgG were highest in PopD (mean 7.92 ± 7.41 and 7.51 ± 9.98, respectively) compared with PopB (mean 4.09 ± 2.81 and 2.30 ± 2.14, respectively) or PopA (mean 1.12 ± 1.08 and 0.97 ± 2.46, respectively) (Fig. 2e). In contrast, the percentage of S2P IgG per total IgG was lower in PopD (mean 0.12 ± 0.20) compared with PopA (mean 0.31 ± 0.62) and especially with PopB (mean 2.46 ± 1.83).

Of eight individuals, the fold change in PopD for Flu:S2P was 66.5 and for Tet:S2P was 63.1 (Supplementary Table 1). In comparison, the fold change within PopB for Flu:S2P was 1.7 and for Tet:S2P was 0.9, demonstrating similar quantities of IgG to Flu, Tet and S2P in PopB. Within the S2P specificity, the fold changes of S2P IgG levels in the BM culture supernatants for PopA:PopD and PopB:PopD were 2.6 and 20.1, respectively (Supplementary Table 2). In comparison, for Flu or Tet specificities, these fold changes were ≤0.31. Ultimately, using this method of measuring secreted antibodies from the cultured BM ASCs, the ratios of non-LLPC:LLPC for Flu, Tet and S2P from BM ASC culture supernatant were 0.66, 0.44 and 23.26, which was similar to the ELISpot results (Fig. 2f). In all, we validate the antigen specificities observed by the ELISpots using our novel in vitro plasma cell culture methods that also showed exclusion of SARS-CoV-2-specific ASCs in PopD.

No correlation of S2P BM ASC responses and time from first vaccine

Because the time from vaccination to BM aspiration varied among the subjects, we compared the time from the last Flu and Tet vaccine as well as from the first SARS-CoV-2 vaccine with the vaccine-specific BM ASC responses. For Flu and Tet, we saw no correlation between the frequencies of vaccine-specific BM ASC subsets (including PopD) with the time windows since the last Flu or Tet vaccine ($R^2 ≤ 0.16$, $P ≥ 0.10$; Extended Data Fig. 5a,b). Similarly, the S2P BM LLPC and non-LLPC frequencies did not correlate with the time from the first vaccine ($R^2 ≤ 0.07$, $P ≥ 0.29$; Extended Data Fig. 5c), the number of vaccine doses ($R^2 ≤ 0.05$, $P ≥ 0.39$; Extended Data Fig. 6) or age of BM subjects ($R^2 ≤ 0.03$, $P ≥ 0.50$; Extended Data Fig. 7). These results suggest that more time since SARS-CoV-2 mRNA vaccination or more vaccine doses does not necessarily promote more S2P PopD responses (in our small cohort).

No differences in BM ASC after vaccine or vaccine with infection

We next compared the S2P BM ASC frequencies in SARS-CoV-2 infected subjects who were also vaccinated ($n = 5$) with those who were only vaccinated with no self-reported infection ($n = 14$). Between these two groups, we found no differences in S2P LLPC and non-LLPC responses—stratified either by the time from the first ($R^2 ≤ 0.10$, $P ≥ 0.32$; Extended Data Fig. 8a) or the last ($R^2 ≤ 0.19$, $P ≥ 0.49$; Extended Data Fig. 8b) vaccine. Although the small number of samples made it difficult to draw definitive conclusions, these results suggest that SARS-CoV-2 infection may also fail to elicit BM LLPCs.

Declined serum S2P, not Flu, Tet or total, IgG

To assess the kinetics of serum antibodies, we measured total IgG as well as Flu, Tet and S2P IgG responses up to 38 months after the first
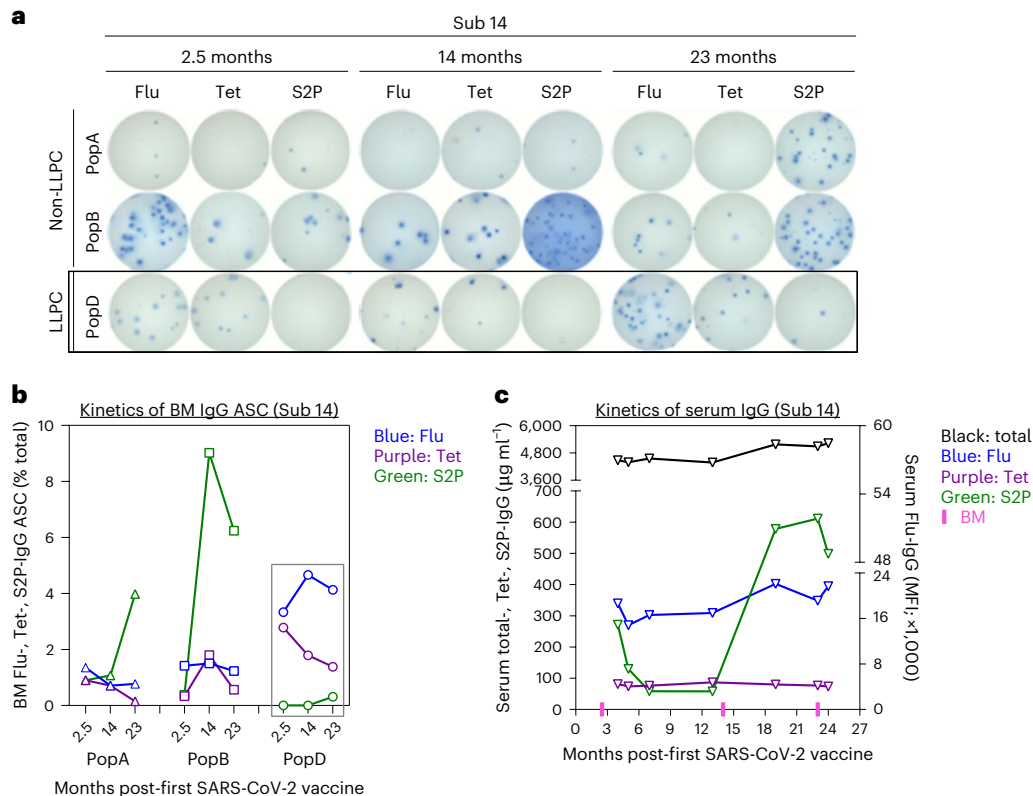
Fig. 4 | Kinetics and magnitude of BM IgG ASC responses and of total and vaccine-specific serum IgG levels in the subject who donated three longitudinal BM aspirates over 2 years (subject 14). a, ELISpot scanned images. The numbers of input ASC that were incubated were ~21K, ~40K and ~4.9K (2.5 months); ~14K, ~12K and ~3.8K (14 months); and ~58K, ~22K and ~7.2K (23 months) for PopA, PopB and PopD, respectively. **b**,**c**, The kinetics and magnitude of antigen-specific BM IgG ASC responses (**b**) and of total and

antigen-specific IgG levels in the serum (**c**). Sera were collected within 1–5 months of the time of BM aspiration. Part of Fig. 4c is reproduced from Fig. 3a for the purpose of kinetics comparison. Sub, subject; K, 1,000. Counts were provided by the sorters. LLPC, boxes in **a** and **b**. All serum samples were tested at dilutions of 1:1,000–1:100,000 (total IgG) or 1:200–1:16,000 (antigen-specific IgG). For serum total and vaccine-specific IgG standard curves, see Supplementary Fig. 1. For details of subjects and samples, see Table 1.

SARS-CoV-2 vaccine. From subjects with at least two sequential serum samples collected within 5 months of the time of BM aspiration (*n* = 8), we observed a decline of S2P IgG titers in the serum within 3–6 months post-first SARS-CoV-2 vaccine (Fig. 3a). One subject had a booster at 7 months after the first SARS-CoV-2 vaccine (subject 8) that showed a rise and a rapid fall in antibody titers. While total IgG and Flu and Tet IgG titers in the serum were relatively stable during the period of 38 months after the first SARS-CoV-2 vaccine in this cohort, serum S2P IgG levels declined within 3–6 months of vaccination unless boosted by additional SARS-CoV-2 vaccines.

### Correlation of serum S2P IgG and BM IgG non-LLPCs
To investigate the relationship between systemic antibodies and BM ASC responses, we analyzed the IgG titers in the serum and the frequencies of BM IgG ASCs (which include LLPCs, non-LLPCs and the sum of both as the total vaccine-specific ASCs). We saw a modest correlation between serum Flu IgG and total BM Flu IgG ASCs ($R^2 = 0.35$, $P < 0.01$; Fig. 3b). When separating LLPCs and non-LLPCs from the total vaccine-specific ASCs, there were also modest correlations of serum Flu IgG titers with BM Flu IgG non-LLPCs ($R^2 = 0.35$, $P = 0.02$) or with LLPCs ($R^2 = 0.43$, $P < 0.01$). Interestingly, for Tet, we observed a very strong correlation between serum IgG titers and BM IgG LLPCs ($R^2 = 0.83$, $P < 0.01$) or total ASCs ($R^2 = 0.78$, $P < 0.01$) but not non-LLPCs ($R^2 < 0.01$, $P = 0.91$) (Fig. 3c). On the contrary, for S2P, we found a significant correlation between serum IgG levels and BM IgG non-LLPCs or total ASCs ($R^2 = 0.52$, $P < 0.01$ or $R^2 = 0.49$, $P < 0.01$, respectively) but no correlation for LLPCs ($R^2 = 0.02$, $P = 0.61$) (Fig. 3d). Together, these results show that serum Tet and Flu but not S2P IgG levels largely

correlate with the vaccine-specific BM IgG LLPC responses; in contrast, serum IgG levels for S2P specificity are associated with the S2P BM IgG non-LLPC frequencies.

Kinetic responses for IgG ASCs in longitudinal BM aspirates
We next assessed the IgG ASC kinetic responses in a subject (subject 14) who provided three sequential BM aspirates over a period of 23 months. BM aspirates were taken 2.5, 14 and 23 months after the first SARS-CoV-2 vaccine (Table 1). Seven serum samples were collected within months of each BM aspiration. Each BM aspirate provided >3,000 FACS-sorted ASCs in each subset. Again, total IgG ASCs were detected in all BM PopA, PopB and PopD. We observed an increase in the frequencies of S2P IgG ASCs in PopA and PopB at 14 months (1.07% and 9.02%, respectively) and 23 months (3.98% and 6.24%, respectively), compared with the first time point (0.90% and 0.38%, respectively) (Fig. 4a,b). However, in PopD, there were no S2P IgG ASCs detected at the first two time points and only 0.31% at the last one (23 months). Notably, at the earliest time point (2.5 months), the highest S2P IgG ASC frequency was observed in PopA, then at both later time points (14 months and 23 months), it was highest in PopB. In all, regardless of time points, the S2P ASC frequencies were always higher in PopA and PopB compared with PopD (even at 23 months). We observed the highest Flu and Tet frequencies in PopD, followed by PopB, and lowest in PopA. Interestingly, the Flu and Tet BM ASC frequencies were quite consistent over the course of 2 years.

In the serum, as expected, total IgG as well as Flu and Tet IgG levels were stable during the examined time periods (Fig. 4c). In contrast, after an initial decline within 3–6 months after SARS-CoV-2 vaccination, S2P IgG titers remained at low levels for about seven months. They then
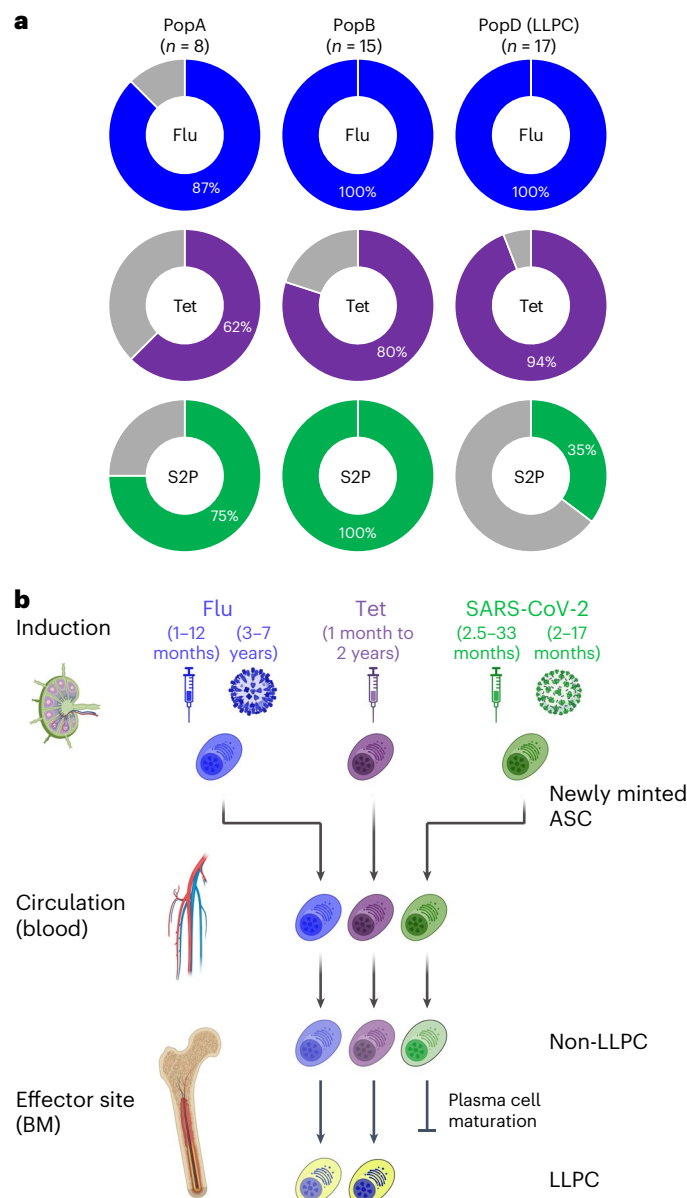
Fig. 5 | **SARS-CoV-2 BM IgG LLPCs are not durably established after mRNA vaccination. a**, Antigen specificity strata of all individuals examined for each BM ASC subset. *n*, number of BM donors. **b**, Graphical summary. The majority of SARS-CoV-2 plasma cells are not established from the BM LLPC compartment 33 months after mRNA vaccination. Created with BioRender.com.

ASC responses were consistently higher in PopA and PopB compared with PopD, suggesting S2P ASCs are not established in the BM LLPC compartment after almost 3 years since the primary SARS-CoV-2 mRNA vaccination.

Few subjects show S2P BM LLPC at low frequencies

Finally, when we calculated the number of individuals with S2P-positive responses for each BM ASC subset, S2P IgG ASCs were easily detected in PopA in 6/8 (75%) individuals and in PopB, in all 15/15 (100%) subjects (Fig. 5a). Only 6/17 (35.29%) subjects had S2P IgG ASCs in PopD, and all were extremely low frequencies despite four or five doses of the vaccine and multiple known SARS-CoV-2 infections. As expected, nearly all subjects had easily detectable Flu and Tet specificities in PopD: 17/17 (100%) and 16/17 (94.12%) respectively. Altogether, durable serologic immune response correlates well with the abundance of Flu and Tet BM ASCs in PopD, while short-lived serologic antibody responses to SARS-CoV-2 mRNA vaccines may be explained by the exclusion of S2P ASCs from this compartment (summarized in Fig. 5b).

Discussion

In this study, we show that SARS-CoV-2 ASCs in the BM are largely excluded from the LLPC compartment. This phenomenon is in stark contrast to Flu and Tet specificities which are inherent to the BM LLPCs. These results highlight the importance of BM maturation programs, where an early-minted ASC undergoes dramatic morphological, transcriptional and epigenetic modifications together with metabolic alterations, to undergo final maturation steps to become a LLPC[5,11]. Increased Ig transcripts[12] and increased unfolded protein response[35], anti-apoptotic[11] and autophagy[36] programs are a few of the pathways involved in ASC maturation[37]. Because this progression is arduous, not all the new arrivals can ultimately complete the entire LLPC process. Thus, dissecting the detailed mechanisms of the LLPC maturation programs will be important.

At one time, it was thought that all human ASCs had the potential to become LLPCs by simply migrating to environments rich in survival factors. However, recent evidence shows how imprinting of an early-minted ASCs at the time of priming in addition to terminal maturation in survival niches endows particular properties for durability. LLPCs are thought to come from memory B cells[38], especially memory B cells with FcRL5+ T-bet+ (ref. 39), but with SARS-CoV-2 mRNA vaccines, they fail to imprint these LLPC programs even 33 months after the vaccine. Thus, a longer tincture of time is unlikely to fill the LLPC subset, but more studies are needed.

There are two explanations for the abundant S2P specificity in PopA at 23 months as well as PopB at 14 and 23 months in the patient with sequential BM aspirates 2 years after the vaccine. Conventionally, PopA and PopB are the result of more recent immune responses, and so breakthrough asymptomatic infections[40–42] (which were well described with the emergence of the highly transmissible Omicron variants[43–45]) temporally close to the corresponding BM sampling may explain these higher S2P frequencies. Nonetheless, even 23 months after vaccination and infection(s), S2P ASCs still cannot fill the BM LLPC compartment. A second explanation is that lymph node S2P ASCs, a product of ongoing germinal center (GC) reactions that can last for 6 months after vaccination[30,31], continue to migrate to the BM. However, this argument still emphasizes the fact that, even 2 years after the vaccine, PopB cannot differentiate into LLPC even with ongoing GC reactions.

Our results are consistent with recent BM studies by Tehrani et al.[46] demonstrating that most SARS-CoV-2 spike-specific ASCs are detectable in the CD19+ compartments after SARS-CoV-2 infection alone. In this study, BM sampling occurred only 5–8 months post-illness and not up to 3 years as in our study, and they used frozen BM ASCs with limited viability upon thawing[46]. Also, the authors did not include longitudinal samples, IgA isotypes, Flu specificity or PopA. Nonetheless, 5–8 months

increased significantly, corresponding to the high frequencies of S2P PopB in the BM at 14 months and 23 months (Fig. 4b). Importantly, this increase occurred without any additional SARS-CoV-2 vaccination and stayed elevated for about 6 months, suggesting asymptomatic and/or unreported infections.

In a second subject (subject 19) with two sequential BM aspirates collected at 28 months and 33 months after the first SARS-CoV-2 vaccine (Table 1), the vaccine-specific IgG ASC responses in the BM were quite similar: the highest frequency of S2P ASCs was found in PopB (3.25% and 3.34%), followed by PopA (0.46% and 0.35%) and PopD (0.40% and 0.33%) (Extended Data Fig. 9a,b). During this period, Flu and Tet BM ASC responses remained stable with the highest in PopD (Flu: 14.28% and 13.68%, and Tet: 3.97% and 3.67%, respectively) compared with PopB (Flu: 4.11% and 4.05%, and Tet: 0.43% and 0.24%, respectively) and PopA (Flu: 1.86% and 1.74%, and Tet: 0% and 0%, respectively). Thus, analysis of longitudinal BM aspirates demonstrates that S2P BM IgG

after infection alone, SARS-CoV-2 ASCs still appear to be absent from the BM LLPC compartment, similar to our findings after vaccination.

In another flow cytometry-based BM study, Schulz et al. found predominate SARS-CoV-2 S1-specific responses in the BM CD19^{+} ASC compartment after 17 months after vaccination[47]. The authors noted some specificity in the CD19^{neg} ASC compartment and concluded they are long-lived. However, these specific ASCs are notably in the CD45^{+} (of CD19^{neg}) ASC subset[47], and the majority of LLPC demonstrate downregulation of CD45[10,48,49] (Extended Data Fig. 10). In concordance with our findings, in Schulz et al.[47], the CD19^{neg}CD45^{neg} subset, which includes the majority of our previously defined LLPCs, also excludes SARS-CoV-2 responses. Hence, the bona fide LLPC, which may be a subset of the CD19^{neg} BM ASC population, probably harbors Flu, Tet, measles and mumps specificities[10] but excludes SARS-CoV-2 responses.

We cannot rule out the possibility where a subset of PopB may be an intermediary population on the road to LLPC maturation. Our previous single-cell transcriptional data showed that the most mature BM ASC clusters with aggregated LLPC also contain PopB[12]. Thus, simple surface markers CD19 and CD138 may be too blunt to dissect the heterogeneity of PopB, which includes new arrivals as well as early mature subsets. Ultimately, dissection into the transcriptional and epigenetic differences in Tet versus S2P PopB (CD19^{+}CD138^{+}) may reveal important mechanistic differences in the formation of long-lived ASCs.

Although the emergence of new SARS-CoV-2 variants of confounded serum protection, we focused on responses against the original virus and the wild-type vaccines, knowing that they rapidly wane within 3–6 months regardless of the vaccine platform (mRNA or adenovirus (Ad) vectors)[3,4]. Interestingly, the Ad vectors persist for weeks, yet specific humoral immunity is also short-lasting[3,4]. Given that both the mRNA and Ad vector vaccine platforms induce strong GC reactions and interactions with T follicular helper (Tfh) cells, the mechanisms underlying their failure to generate LLPCs are even more puzzling[2] and suggest dysfunction in the maturation process in the BM.

Could the limited durability of neutralizing antibody responses be due to the widely spaced structural nature of the spike protein itself and, thus, limited only to coronavirus vaccines? Coronaviruses lack highly repetitive organized structures or pathogen-associated structural patterns[50]. Most RNA viruses that induce long-lasting antibody immunity have on their surface rigid repetitive structures spaced at 5–10 nm (ref. 51). For coronaviruses, the long spike proteins are embedded in a fluid membrane, which are often loosely floating and widely spaced at 25 nm apart[50]. Therefore, the inherent nature of the spike protein itself may be an issue in B cell activation[51] since neutralizing antibody responses to seasonal human coronaviruses, as well as to SARS-CoV-1 and MERS-CoV, are also short-lived[2].

There are limitations in our study. First, our sample size is relatively small, especially those after both vaccination and infection. Second, the infections were self-reported symptoms that warranted testing, so any asymptomatic infections were not confirmed. Third, primary BM ASCs are rare cell types and BM aspirates are difficult to obtain and interrogate; thus, not all samples provided sufficient cells for each BM subset. Fourth, we had limited longitudinal and sequential samples with the longest at 33 months since the first SARS-CoV-2 vaccine. Lastly, in this cohort, the modest correlation between serum Flu IgG and total BM Flu IgG ASC may not only reflect Flu-specific responses elicited by the last Flu vaccine but also exhibit cross-reactivity to older Flu strains[23]. Thus, it would also be important to assess the BM compartments decades after the primary vaccines as new variant SARS-CoV-2 viruses continue to emerge and circulate.

In conclusion, the holy grail of vaccinology is the generation of LLPCs. Our findings demonstrate the exclusion of SARS-CoV-2 specificity in the BM LLPCs and the need to improve durability of the mRNA vaccines. Whether optimizing vaccine regimens or immunization schedules, engineering different spike proteins or formulating vaccine adjuvants and delivery systems will need better understanding.

Online content

Any methods, additional references, Nature Portfolio reporting summaries, source data, extended data, supplementary information, acknowledgements, peer review information; details of author contributions and competing interests; and statements of data and code availability are available at https://doi.org/10.1038/s41591-024-03278-y.

References

1. WHO. WHO COVID-19 dashboard. https://covid19.who.int (2024).
2. Nguyen, D. C. et al. COVID-19 and plasma cells: is there long-lived protection? *Immunol. Rev.* **309**, 40–63 (2022).
3. Bhattacharya, D. Instructing durable humoral immunity for COVID-19 and other vaccinable diseases. *Immunity* **55**, 945–964 (2022).
4. Lasrado, N. & Barouch, D. H. SARS-CoV-2 hybrid immunity: the best of both worlds. *J. Infect. Dis.* https://doi.org/10.1093/infdis/jiad353 (2023).
5. Nguyen, D. C. et al. Plasma cell survival: the intrinsic drivers, migratory signals, and extrinsic regulators. *Immunol. Rev.* **303**, 138–153 (2021).
6. Nguyen, D. C. et al. Majority of human circulating IgG plasmablasts stop blasting in a cell-free pro-survival culture. *Sci. Rep.* **14**, 3616 (2024).
7. Turner, J. S. et al. SARS-CoV-2 infection induces long-lived bone marrow plasma cells in humans. *Nature* https://doi.org/10.1038/s41586-021-03647-4 (2021).
8. Kim, W. et al. Germinal centre-driven maturation of B cell response to mRNA vaccination. *Nature* **604**, 141–145 (2022).
9. Prabhakaran, M. et al. Adjuvanted SARS-CoV-2 spike protein vaccination elicits long-lived plasma cells in nonhuman primates. *Sci. Transl. Med.* **16**, eadd5960 (2024).
10. Halliley, J. L. et al. Long-lived plasma cells are contained within the CD19^{-}CD38^{hi}CD138^{+} subset in human bone marrow. *Immunity* **43**, 132–145 (2015).
11. Joyner, C. J. et al. Generation of human long-lived plasma cells by developmentally regulated epigenetic imprinting. *Life Sci. Alliance* https://doi.org/10.26508/lsa.202101285 (2022).
12. Duan, M. et al. Understanding heterogeneity of human bone marrow plasma cell maturation and survival pathways by single-cell analyses. *Cell Rep.* **42**, 112682 (2023).
13. Liu, X., Yao, J., Zhao, Y., Wang, J. & Qi, H. Heterogeneous plasma cells and long-lived subsets in response to immunization, autoantigen and microbiota. *Nat. Immunol.* **23**, 1564–1576 (2022).
14. Robinson, M. J. et al. Intrinsically determined turnover underlies broad heterogeneity in plasma-cell lifespan. *Immunity* **56**, 1596–1612 e1594 (2023).
15. Mei, H. E. et al. A unique population of IgG-expressing plasma cells lacking CD19 is enriched in human bone marrow. *Blood* **125**, 1739–1748 (2015).
16. Nguyen, D. C. et al. Factors of the bone marrow microniche that support human plasma cell survival and immunoglobulin secretion. *Nat. Commun.* **9**, 3698 (2018).
17. Nguyen, D. C., Joyner, C. J., Sanz, I. & Lee, F. E. Factors affecting early antibody secreting cell maturation into long-lived plasma cells. *Front. Immunol.* **10**, 2138 (2019).
18. Tellier, J. & Nutt, S. L. The secret to longevity, plasma cell style. *Nat. Immunol.* **23**, 1507–1508 (2022).
19. Amanna, I. J., Carlson, N. E. & Slifka, M. K. Duration of humoral immunity to common viral and vaccine antigens. *N. Engl. J. Med.* **357**, 1903–1915 (2007).
20. Krammer, F. The human antibody response to influenza A virus infection and vaccination. *Nat. Rev. Immunol.* **19**, 383–397 (2019).
21. Halasa, N. B., Gerber, M. A., Chen, Q., Wright, P. F. & Edwards, K. M. Safety and immunogenicity of trivalent inactivated influenza vaccine in infants. *J. Infect. Dis.* **197**, 1448–1454 (2008).

22. Bodewes, R. et al. Prevalence of antibodies against seasonal influenza A and B viruses in children in Netherlands. *Clin. Vaccin. Immunol.* **18**, 469–476 (2011).

23. Kucharski, A. J. et al. Estimating the life course of influenza A(H3N2) antibody responses from cross-sectional data. *PLoS Biol.* **13**, e1002082 (2015).

24. Hancock, K. et al. Cross-reactive antibody responses to the 2009 pandemic H1N1 influenza virus. *N. Engl. J. Med.* **361**, 1945–1952 (2009).

25. Katz, J. et al. Serum cross-reactive antibody response to a novel influenza A (H1N1) virus after vaccination with seasonal influenza vaccine. *MMWR Morb. Mortal. Wkly Rep.* **58**, 521–524 (2009).

26. Skountzou, I. et al. Immunity to pre-1950 H1N1 influenza viruses confers cross-protection against the pandemic swine-origin 2009 A (H1N1) influenza virus. *J. Immunol.* **185**, 1642–1649 (2010).

27. Fisman, D. N. et al. Older age and a reduced likelihood of 2009 H1N1 virus infection. *N. Engl. J. Med.* **361**, 2000–2001 (2009).

28. Nachbagauer, R. et al. Defining the antibody cross-reactome directed against the influenza virus surface glycoproteins. *Nat. Immunol.* **18**, 464–473 (2017).

29. Yu, X. et al. Neutralizing antibodies derived from the B cells of 1918 influenza pandemic survivors. *Nature* **455**, 532–536 (2008).

30. Wrammert, J. et al. Rapid cloning of high-affinity human monoclonal antibodies against influenza virus. *Nature* **453**, 667–671 (2008).

31. Lee, F. E. et al. Circulating human antibody-secreting cells during vaccinations and respiratory viral infections are characterized by high specificity and lack of bystander effect. *J. Immunol.* **186**, 5514–5521 (2011).

32. Wrapp, D. et al. Cryo-EM structure of the 2019-nCoV spike in the prefusion conformation. *Science* **367**, 1260–1263 (2020).

33. Odendahl, M. et al. Generation of migratory antigen-specific plasma blasts and mobilization of resident plasma cells in a secondary immune response. *Blood* **105**, 1614–1621 (2005).

34. Haddad, N. S. et al. One-stop serum assay identifies COVID-19 disease severity and vaccination responses. *Immunohorizons* **5**, 322–335 (2021).

35. Tellier, J. et al. Blimp-1 controls plasma cell function through the regulation of immunoglobulin secretion and the unfolded protein response. *Nat. Immunol.* **17**, 323–330 (2016).

36. Pengo, N. et al. Plasma cells require autophagy for sustainable immunoglobulin production. *Nat. Immunol.* **14**, 298–305 (2013).

37. Lam, W. Y. et al. Metabolic and transcriptional modules independently diversify plasma cell lifespan and function. *Cell Rep.* **24**, 2479–2492 e2476 (2018).

38. Palm, A. E. & Henry, C. Remembrance of things past: long-term B cell memory after infection and vaccination. *Front. Immunol.* **10**, 1787 (2019).

39. Nellore, A. et al. A transcriptionally distinct subset of influenza-specific effector memory B cells predicts long-lived antibody responses to vaccination in humans. *Immunity* **56**, 847–863 e848 (2023).

40. White, E. M. et al. Asymptomatic and presymptomatic severe acute respiratory syndrome coronavirus 2 infection rates in a multistate sample of skilled nursing facilities. *JAMA Intern. Med.* **180**, 1709–1711 (2020).

41. Shang, W. et al. Percentage of asymptomatic infections among SARS-CoV-2 Omicron variant-positive individuals: a systematic review and meta-analysis. *Vaccines* https://doi.org/10.3390/vaccines10071049 (2022).

42. El-Ghitany, E. M. et al. Asymptomatic versus symptomatic SARS-CoV-2 infection: a cross-sectional seroprevalence study. *Trop. Med Health* **50**, 98 (2022).

43. Garrett, N. et al. High asymptomatic carriage with the omicron variant in South Africa. *Clin. Infect. Dis.* **75**, e289–e292 (2022).

44. Christensen, P. A. et al. Signals of significantly increased vaccine breakthrough, decreased hospitalization rates, and less severe disease in patients with coronavirus disease 2019 caused by the omicron variant of severe acute respiratory syndrome coronavirus 2 in Houston, Texas. *Am. J. Pathol.* **192**, 642–652 (2022).

45. Oran, D. P. & Topol, E. J. Prevalence of asymptomatic SARS-CoV-2 infection: a narrative review. *Ann. Intern. Med.* **173**, 362–367 (2020).

46. Tehrani, Z. R. et al. Deficient generation of spike-specific long-lived plasma cells in the bone marrow after severe acute respiratory syndrome coronavirus 2 infection. *J. Infect. Dis.* https://doi.org/10.1093/infdis/jiad603 (2024).

47. Schulz, A. R. et al. SARS-CoV-2 specific plasma cells acquire long-lived phenotypes in human bone marrow. *EBioMedicine* **95**, 104735 (2023).

48. Mujtahedi, S. S. et al. Bone marrow derived long-lived plasma cell phenotypes are heterogeneous and can change in culture. *Transpl. Immunol.* **75**, 101726 (2022).

49. Pellat-Deceunynck, C. & Bataille, R. Normal and malignant human plasma cells: proliferation, differentiation, and expansions in relation to CD45 expression. *Blood Cells Mol. Dis.* **32**, 293–301 (2004).

50. Bachmann, M. F., Mohsen, M. O., Zha, L., Vogel, M. & Speiser, D. E. SARS-CoV-2 structural features may explain limited neutralizing-antibody responses. *NPJ Vaccines* **6**, 2 (2021).

51. Slifka, M. K. & Amanna, I. J. Role of multivalency and antigenic threshold in generating protective antibody responses. *Front. Immunol.* **10**, 956 (2019).

[1]Division of Pulmonary, Allergy, Critical Care, and Sleep Medicine, Department of Medicine, Emory University, Atlanta, GA, USA. [2]Division of Rheumatology, Department of Medicine, Emory University, Atlanta, GA, US. [3]Department of Hematology and Medical Oncology, Winship Cancer Institute, Emory University, Atlanta, GA, USA. [4]Lowance Center for Human Immunology, Emory University, Atlanta, GA, USA. [5]Present address: Department of Medicine, Atlanta Veterans Affairs Healthcare System, Atlanta, GA, USA. ✉e-mail: f.e.lee@emory.edu

Methods

Healthy human subjects

A total of 22 BM aspirate samples were obtained from 19 healthy adult donors who self-reported to receive influenza, Tdap (tetanus, diphtheria and pertussis) and COVID-19 primary and booster vaccines. Serum samples were also collected from all the subjects (one to seven draws per subject) within 5 months (before and/or after) of BM aspiration. Select demographic and clinical characteristics of the subjects can be seen in Fig. 1a. Detailed information on BM subjects and BM aspirates can be found in Table 1. For antigen optimization and selection, peripheral blood samples were obtained from 64 healthy subjects who received vaccines for influenza, Tdap or COVID-19 (the third, fourth or fifth dose) at 5–7 days before sample collection. For CD45 flow cytometric staining, BM aspirates from an addition of five healthy BM subjects were obtained, stained, acquired and analyzed.

Written informed consent was obtained from all subjects. Samples were collected over 3 years to be confident the results were statistically significant to distinguish different biological antigen-specific BM subsets. We recruited adult subjects who are healthy as defined by a health survey with no history of autoimmune, renal, liver, cardiopulmonary and vascular disease. Patients with history of malignancy, transplant, human immunodeficiency virus or hepatitis C or those on immunosuppressive therapies are also excluded. The participants were remunerated for the time and inconvenience. All research was approved by the Emory University Institutional Review Board (IRB) Committee (Emory IRB numbers IRB00066294 and IRB00057983) and was performed in accordance with all relevant guidelines and regulations.

Purification of blood and BM ASC

Isolation of peripheral blood mononuclear cells and BM mononuclear cells (BMMCs) was performed according to our established procedure[16]. Briefly, mononuclear cells were isolated by Ficoll density gradient centrifugation and enriched by either a commercial human Pan-B cell enrichment kit (that removes cells expressing CD2, CD3, CD14, CD16, CD36, CD42b, CD56, CD66b, CD123 and glycophorin A) (StemCell Technologies) or a custom-designed negative selection cell isolation kit (that removes cells expressing CD3, CD14, CD66b and glycophorin A) (StemCell Technologies) to limit sorting time and pressure on fragile ASCs. For the ASC sorting panels, cell-enriched fractions from blood or BM aspirates were stained with the following anti-human antibodies: IgD–FITC (cat. #555778; BD Biosciences) at 1:5 dilution or IgD-BV480 (cat. #566138; BD Biosciences) at 1:5 dilution, CD3-BV711 (cat. #317328; BioLegend) at 1:20 dilution or CD3-BUV737 (cat. #612750; BD Biosciences) at 1:20 dilution, CD14-BV711 (cat. #301838; BioLegend) at 1:20 dilution or CD14-BUV737 (cat. #612763; BD Biosciences) at 1:20 dilution, CD19-PE-Cy7 (cat. #560911; BD Biosciences) at 1:5 dilution or CD19-Spark NIR 685 (cat. #302270; BioLegend) at 1:5 dilution, CD38-V450 (cat. #561378; BD Bioscience) at 1:20 dilution or CD38-BV785 (cat. #303530; BioLegend) at 1:20 dilution, CD138-APC (cat. #130-117-395; Miltenyi Biotech) at 1:20 dilution or CD138-APC-R700 (cat. #566050; BD Biosciences) at 1:20 dilution, CD27-APC-e780 (cat. #5016160; eBiosciences) at 1:20 dilution or CD27-BV711 (cat. #356430; BioLegend) at 1:20 dilution, and LiveDead (cat. #L34966; Invitrogen) at 1:600 dilution or Zombie NIR Fixable Viability Kit (cat. #423106; BioLegend) at 1:500 dilution.

Fresh blood ASC as well as BM ASC subsets, which included PopA, PopB and PopD (LLPC), were purified using FACS-based sorting[10,16]. ASC subsets were sorted on a BD FACSAria II using a standardized sorting procedure with rainbow calibration particles to ensure consistency of sorts among individuals. ASC subsets were sorted as follows[10,11,16]: blood ASC (IgD−CD27hiCD38hi), BM ASC (IgD−CD19+CD38hi), PopA (CD19+IgD−38hiCD138−), PopB (CD19+IgD−CD38hiCD138+) and PopD (CD19−IgD−CD38hiCD138+). Sorted ASC populations were generally 93–99% pure (except for PopA, whose purity was usually 60–75%).

Antigen selection for Ig immunoassays

The following antigens were used for vaccine-specific IgG and IgA capturing: quadrivalent influenza vaccine 2019-20, 2020-21, 2021-22 or 2023-24 (Fluarix Quadrivalent Influenza Vaccine 2019-20, 2020-21, 2021-22 or 2023-24 Formula, respectively; GSK Biologicals/ABO Pharmaceuticals; Afluria Quadrivalent (Seqirus); or Fluzone Quadrivalent (Sanofi Pasteur)), tetanus toxoid, *Clostridium tetani* (Calbiochem/Millipore Sigma or Fina Biosolutions) and SARS-CoV-2 S2P (recombinant SARS-CoV-2 soluble spike trimer protein, lot #P210721.02; Protein Expression Laboratory, Frederick National Laboratory for Cancer Research, Frederick, MD). For relative quantitation of antigen-specific antibody titers, standard curves were generated using monoclonal antibody (mAb) standards of anti-tetanus toxin mAb (clone #TetE3; The Native Antigen Company) and SARS-CoV-2-reactive (spike RBD) mAb (Abeomics). For determining the concentrations of total IgG, purified human IgG (ChromePure human IgG, JacksonImmuno Research Laboratories) was used as a standard.

Blood and BM ASC bulk cultures and ELISpot assays

Human ASC cultures were conducted in mesenchymal stromal/stem cell secretome (ASC survival medium) and in hypoxic conditions (2.5% O$_2$) at 37 °C (ref. 16). This culture system is called plasma cell survival system[52]. IgG and IgA secretion of cultured ASC was assessed by ELISpot assays, which quantitated IgG- and IgA-secreting cells, respectively. These assays used goat anti-human IgG or IgA for total IgG or IgA capturing, respectively, and alkaline phosphatase-conjugated goat anti-human IgG or IgA, respectively, for detection, and were performed according to our established procedure[16]. ELISpot data were collected using the Cellular Technology Limited system, which runs ImmunoSpot 5.0.9.21 software.

MBBA

MBBAs were performed on the supernatants collected from culture of BM ASCs purified from eight individuals who provided sufficient post-sort cells for all three subsets as well as from serum samples drawn from all 19 subjects (10 of whom provided 2–7 sequential sera). For total IgG, biotinylated goat anti-human IgG (Southern Biotech) was conjugated to avidin-coupled MagPlex-avidin microspheres of spectrally distinct regions[53]. For vaccine-specific MBBA, antigens were conjugated to MagPlex microspheres (Luminex) of spectrally distinct regions via standard carbodiimide coupling procedure[34]. MBBAs were performed using a FLEXMAP 3D instrument (Luminex)[34]. All viral protein-coupled microspheres were tested together as a combined multiplex antigen-specific immunoassay, and all anti-human Ig coupled microspheres were tested together as a combined multiplex total Ig immunoassay. Median fluorescence intensity (MFI) using combined or individual detection antibodies was measured using the xPONENT 4.3 software (Luminex) at enhanced photomultiplier tube (PMT) setting. The net MFI was obtained by subtracting the background value. The culture supernatant MFI values were normalized to the relative IgG concentrations (pg ml^{-1}) based on the total human IgG standard curves, followed by normalization of these resultant IgG concentrations (pg ml^{-1}) to the ASC input numbers and duration of culture (days). The MFI normalization and binding curves were performed on the basis of the equations shown in Extended Data Fig. 4 and Supplementary Fig. 1. Data were expressed as the percents or ratios of the titers of antigen-specific IgG to those of total IgG (BM ASC culture supernatants) or as IgG concentrations (µg ml^{-1}) (serum total IgG and Tet and S2P IgG). Since the Flu specificities used (vaccines) had four antigens in combination and there were no mAb standards, we used MFI values as a semi-quantitative measure for assessment of Flu IgG levels in the serum. All the BM ASC culture supernatants were collected after one day in culture of off-sorter BM ASC subsets and were tested undiluted (neat) or 1:2 diluted−except for the total IgG titrations, which were also assayed at further dilutions. All sera were assayed at dilutions of 1:1,000–1:100,000 (total IgG) or 1:200–1:16,000 (antigen-specific IgG).

CD45 BM ASC flow cytometry

BMMCs were isolated according to our established procedure[16] and stained with the following anti-human antibodies: IgD-BV480 (cat. #566138; BD Biosciences) at 1:160 dilution, CD3-BUV737 (cat. #612750; BD Biosciences) at 1:160 dilution, CD14-BUV737 (cat. #612763; BD Biosciences) at 1:160 dilution, CD19-Spark NIR 685 (cat. #302270; BioLegend) at 1:160 dilution, CD38-BV785 (cat. #303530; BioLegend) at 1:160 dilution, CD138-APC-R700 (cat. #566050; BD Biosciences) at 1:320 dilution, CD27-BV711 (cat. #356430; BioLegend) at 1:40 dilution, and CD45-PE-Cy5 (cat. #304009; BioLegend) at 1:160 dilution. Samples were run on a Cytek's Aurora Spectral Flow Cytometer using Cytek SpectroFlo software (v3.0; Cytek Biosciences) and analyzed with the FlowJo v10.8.1 software (FlowJo, LLC).

Statistics

Statistics were assessed using Student's *t*-test (two-tailed unpaired *t*-test) in Excel (Microsoft), and differences were considered significant at *P* values less than 0.05. Correlations were assessed using simple linear regression analysis performed with GraphPad Prism (v8.4.2; GraphPad Software). No adjustments were made for multiple comparisons.

Reporting summary

Further information on research design is available in the Nature Portfolio Reporting Summary linked to this article.

Data availability

There are no restrictions on the availability of experimental data from and of unique materials used in this study. All the data generated and/or analyzed in this study are available from the corresponding author. All unique materials used are readily available from the corresponding author and Emory University. Source data are provided with this paper.

Code availability

No new code was generated in this study.

References

52. Woodruff, M. C. et al. Response under pressure: deploying emerging technologies to understand B-cell-mediated immunity in COVID-19. *Nat. Methods* **19**, 387–391 (2022).
53. Haddad, N. S. et al. Circulating antibody-secreting cells are a biomarker for early diagnosis in patients with Lyme disease. *PLoS ONE* **18**, e0293203 (2023).

Acknowledgements

Author contributions

Conceptualization: D.C.N. and F.E.-H.L. Methodology: D.C.N., I.T.H., A.M.P., D.S., N.S.H. and C.C. Resources and sample acquisition: P.A.L., M.C.R., J.A., D.R., S.L., I.S. and F.E.-H.L. Funding acquisition: F.E.-H.L. and I.S. Supervision: F.E.-H.L. Writing—original draft: D.C.N. and F.E.-H.L. All authors have reviewed, edited and approved the final manuscript.

Competing interests

F.E.-H.L. is the founder of Micro-Bplex, Inc., serves on the scientific board of Be Biopharma, is a recipient of grants from the BMGF and Genentech, Inc., and has served as a consultant for Astra Zeneca. I.S. has consulted for GSK, Pfizer, Kayverna, Johnson & Johnson, Celgene, Bristol Myer Squibb and Visterra. F.E.-H.L., D.C.N. and I.S. are inventors of the patents concerning the plasma cell survival media related to this work (US11124766B2, US11125757B2 and Notice of Allowance issued 8/5/2024 for USPTO Patent Application 17/405,918). The other authors declare no competing interests.

Additional information

Extended data is available for this paper at https://doi.org/10.1038/s41591-024-03278-y.

Supplementary information The online version contains supplementary material available at https://doi.org/10.1038/s41591-024-03278-y.

Correspondence and requests for materials should be addressed to F. Eun-Hyung Lee.

Peer review information *Nature Medicine* thanks David Fooksman and the other, anonymous, reviewer(s) for their contribution to the peer review of this work. Primary Handling Editor: Alison Farrell, in collaboration with the *Nature Medicine* team.

Reprints and permissions information is available at www.nature.com/reprints.
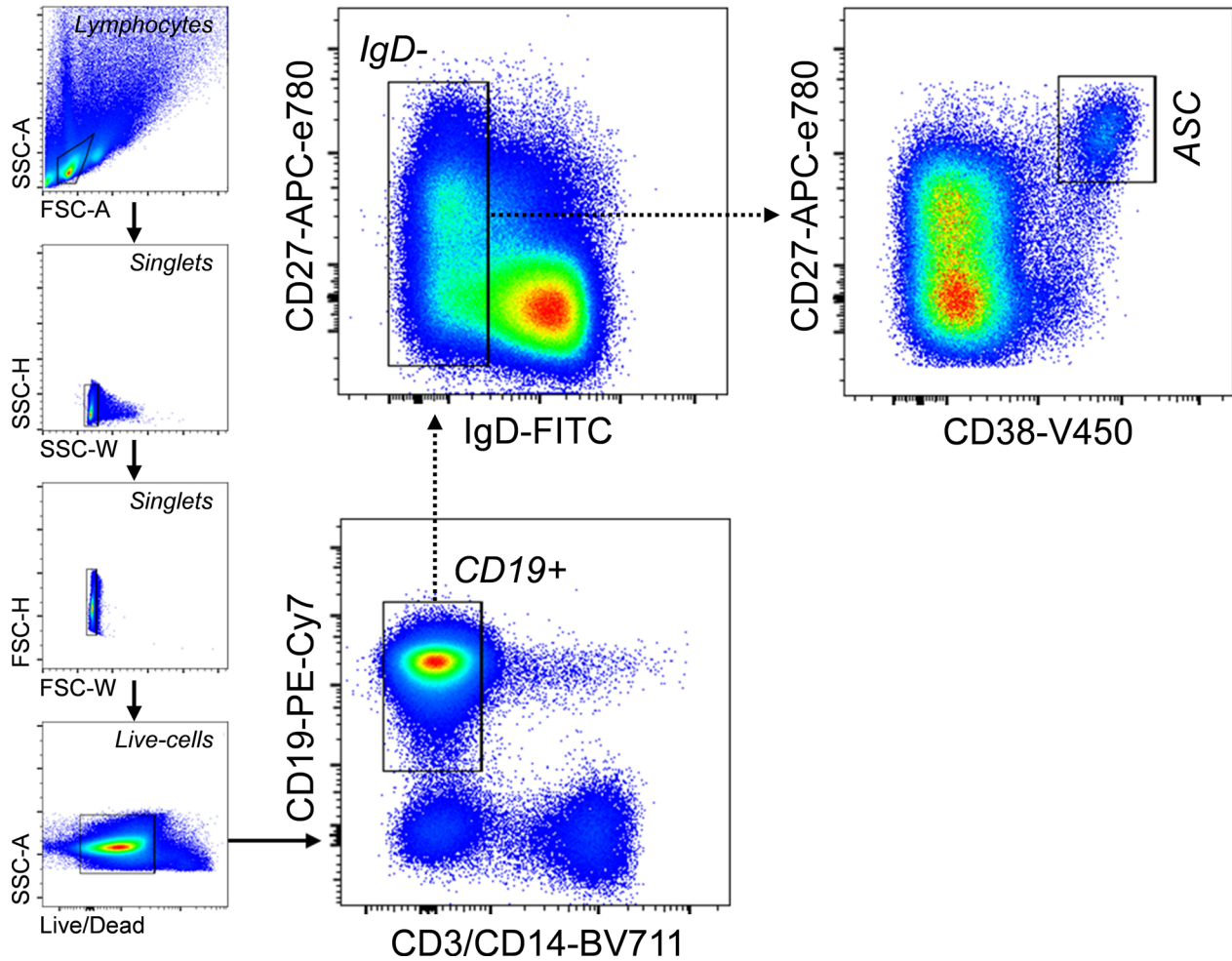
Extended Data Fig. 1 | General FACS gating strategy used for sorting blood ASC. PBMC were first gated for lymphocytes, singlets, and viable cells (based on their FSC/SSC and Live/Death properties). CD3 and CD14 were then used as dump markers to capture CD19+ and CD19⁻ B cell populations. Subsequent sub-gating using CD38 versus CD27 on the IgD- fraction (of CD19+ population) allows for sorting for blood ASC (CD27hiCD38hi). See Methods for antibody panels.
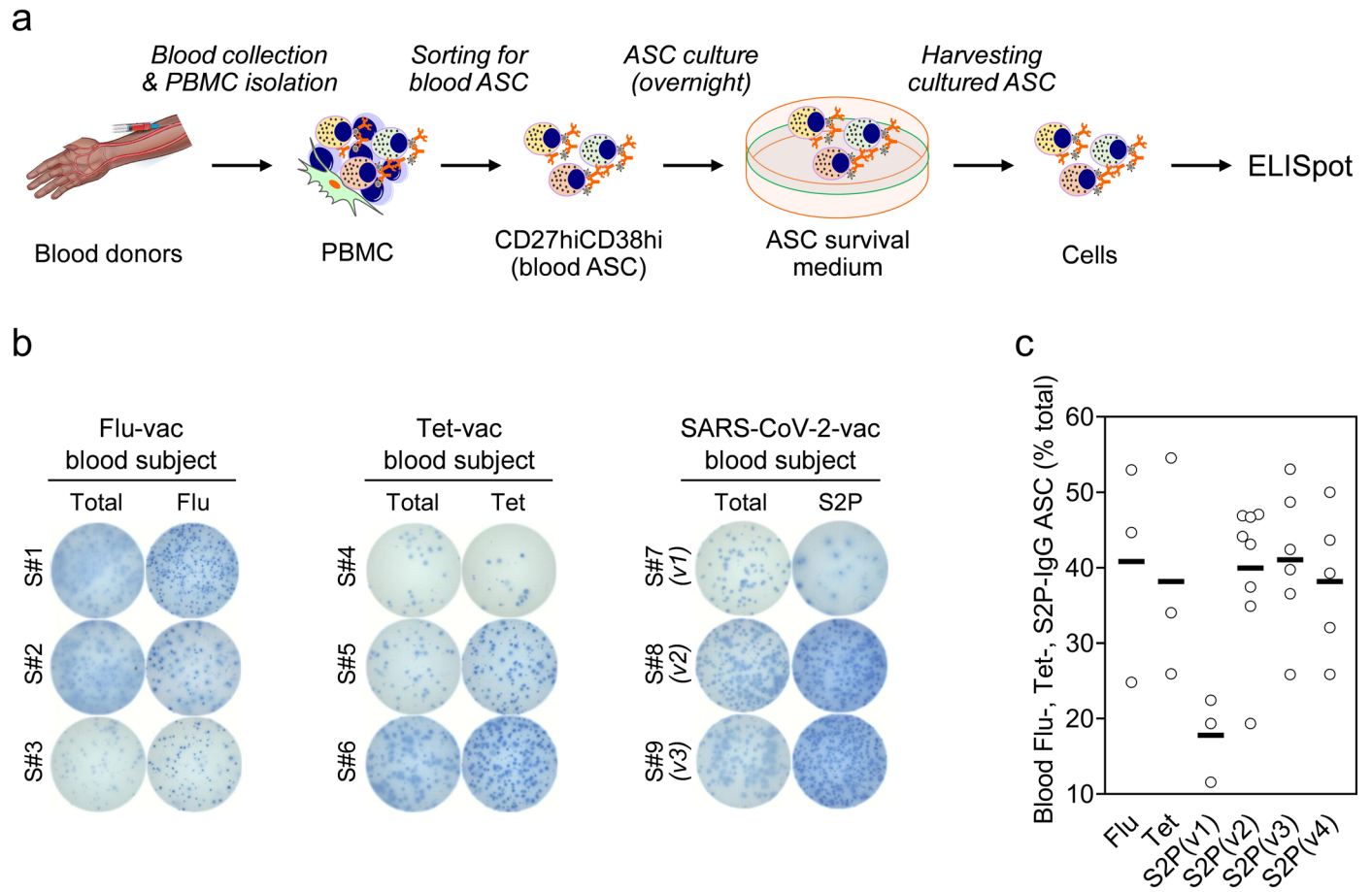
Extended Data Fig. 2 | Assessment of vaccine-specific ASC and validation of vaccine specificities with blood ASC. (a) Summary of the techniques and the experimental designs. From the cultures of blood ASC, the cells were collected and ELISpot-quantitated for validating vaccine specificities. (b) Representative ELISpot scanned images shown. Blood ASC from subjects at the peak (5-7 days post-vaccine) assayed for Flu-, Tet-, and S2P-specific IgG secretion. The numbers of input ASC that were incubated were ~894, ~1,124, and ~796 (total), and ~4,471, ~4,496, and ~2,388 (Flu-specific) for S#1, S#2, and S#3, respectively (far left); ~1 K, ~1 K, and ~1 K (total), and ~3 K, ~4 K, and ~4 K (Tet-specific) for S#4, S#5, and S#6, respectively (left); and ~712, ~1,415, and ~1,386 (total), and ~2,139, ~4,245, and ~5,544 (S2P-specific) for S#7, S#8, and S#9, respectively (right). (c) Each circle represents an individual vaccinee. Data were generated from 3, 3, 3, 8, 6, and 5 different vaccinated subjects for Flu, Tet, S2P (v1), S2P (v2), S2P (v3), and S2P (v4), respectively. S: subject; ~: counts provided by the sorters; K: 1,000; vac: vaccinated; Flu: influenza; Tet: tetanus; v: (SARS-CoV-2 mRNA) vaccine dose. All ASC assayed at day 1 in culture.
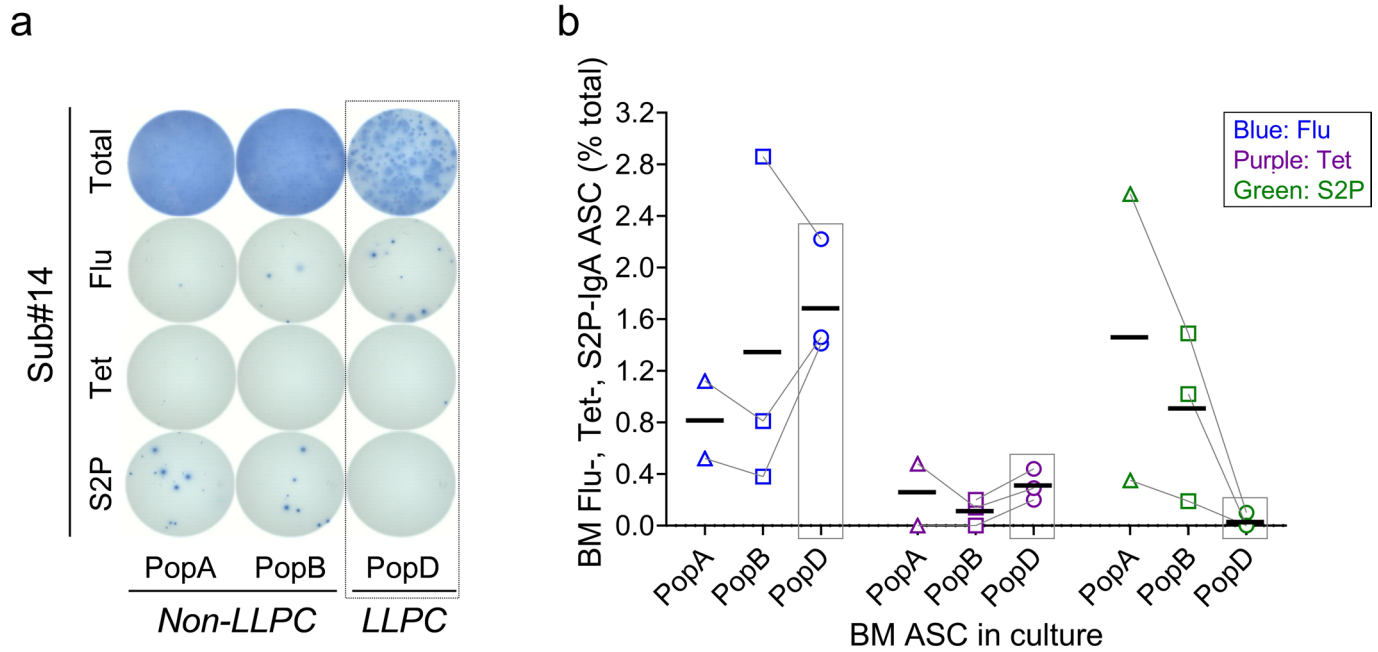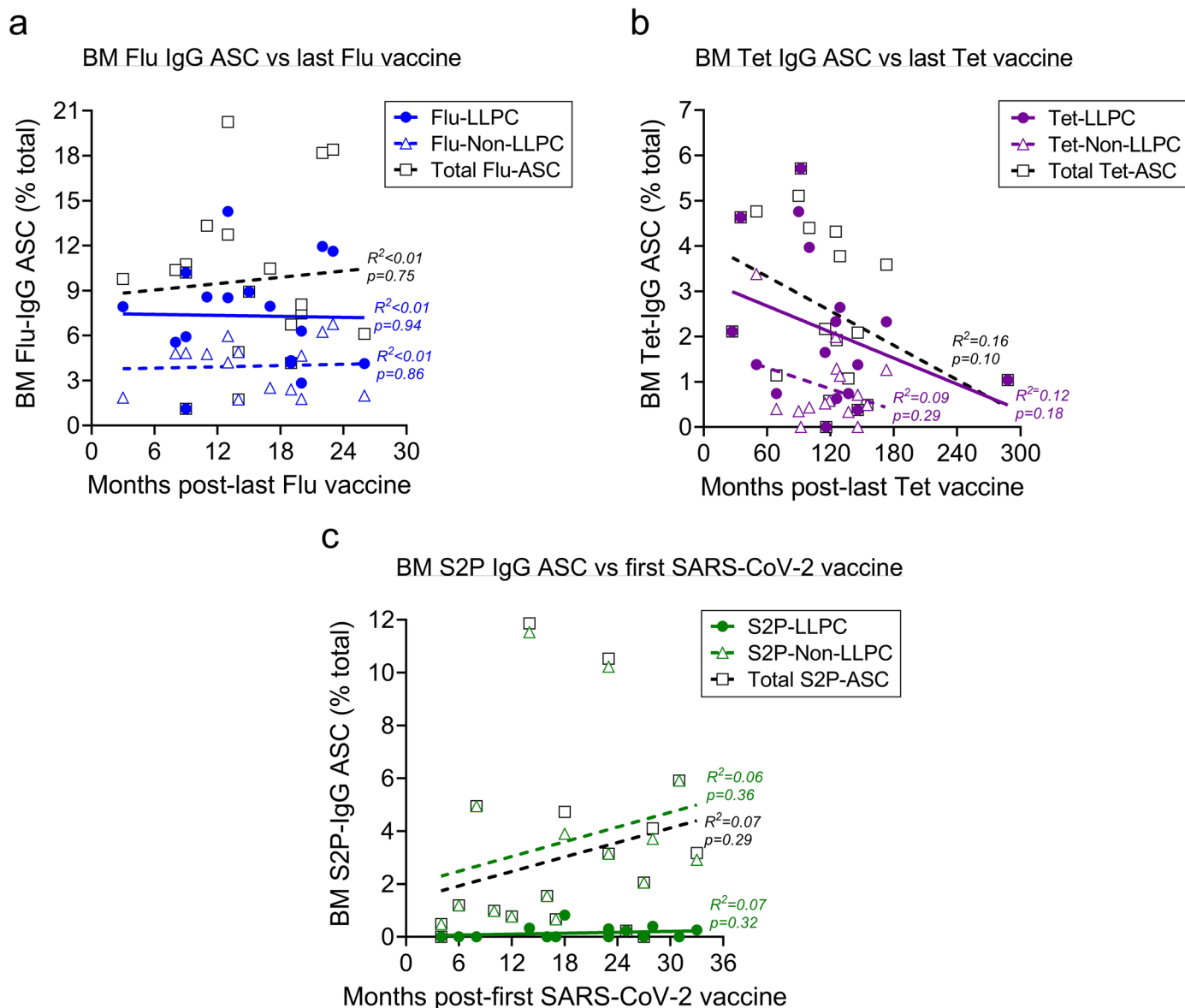
Extended Data Fig. 3 | Exclusion of S2P BM IgA LLPC in SARS-CoV-2 mRNA vaccinees. (**a**) Representative ELISpot scanned images. The numbers of input ASC that were incubated were ~9.6 K, ~3.7 K, and ~1.2 K (total) and ~58 K, ~22 K, and ~7.2 K (vaccine-specific) for PopA, PopB, and PopD, respectively. (**b**) Each symbol represents an individual vaccinee. Data were generated from 2, 3, and 3 different SARS-CoV-2 vaccinated subjects for PopA, PopB, and PopD, respectively. Statistics were assessed using Student's t-test (two-tailed unpaired t-test) in Excel (Microsoft) and differences were considered significant at p values less than 0.05. -: counts provided by the sorters; K: 1,000; LLPC: long-lived plasma cell (dotted boxes); Flu: influenza; Tet: tetanus. All ASC assayed at day 1 in culture. For individual ratios and statistic comparisons between any two antigens for any subset or between any two subsets for any antigen, see Supplementary Tables 3 and 4, respectively.
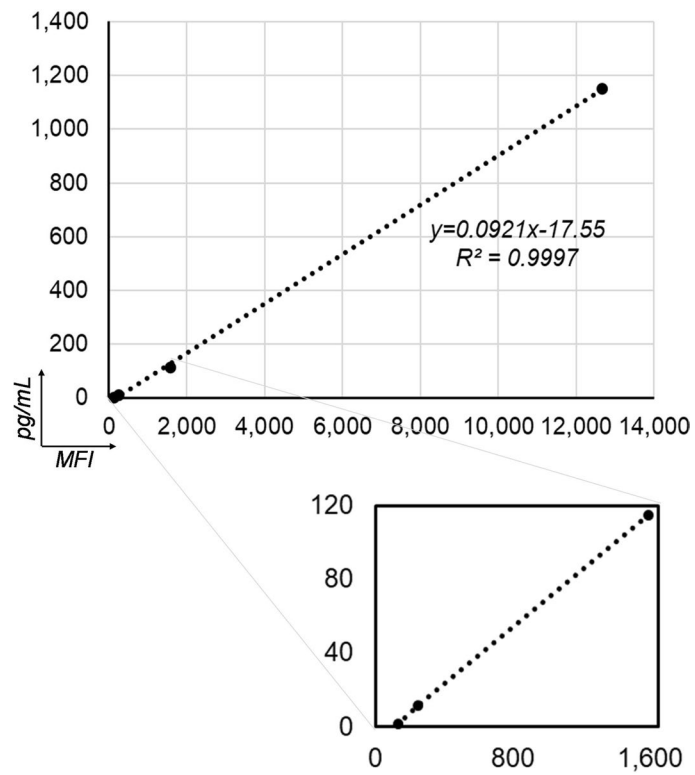
Extended Data Fig. 4 | The human IgG standardized concentrations versus MFI values. The displayed equation was used to normalize MFI values for detection of antibodies in the culture supernatants of each BM ASC subset.

a BM Flu IgG ASC vs last Flu vaccine

b BM Tet IgG ASC vs last Tet vaccine

c BM S2P IgG ASC vs first SARS-CoV-2 vaccine

Extended Data Fig. 5 | No correlation between vaccine-specific IgG BM ASC responses and the time windows of the vaccine. BM (**a**) Flu, (**b**) Tet, and (**c**) S2P IgG LLPC, Non-LLPC, and total ASC responses in all examined subjects following the vaccine exposure time (time since the most recent (**a**) Flu, (**b**) Tet, or (**c**) the first SARS-CoV-2 vaccine). Data were generated from 17, 15, and 19 different SARS-CoV-2 vaccinated subjects for BM LLPC, Non-LLPC, and total ASC, respectively. Correlations were assessed using simple linear regression analysis performed with GraphPad Prism (GraphPad Software). The exact p values for vaccine-specific LLPC, Non-LLPC, and total ASC are 0.9397, 0.8563, and 0.7455, respectively (**a**); 0.1806, 0.2898, and 0.0952, respectively (**b**); and 0.3202, 0.3635, and 0.2862, respectively (**c**). Subjects yielding sufficient ASC for LLPC and Non-LLPC subsets included.

BM S2P IgG ASC vs # SARS-CoV-2 vaccines
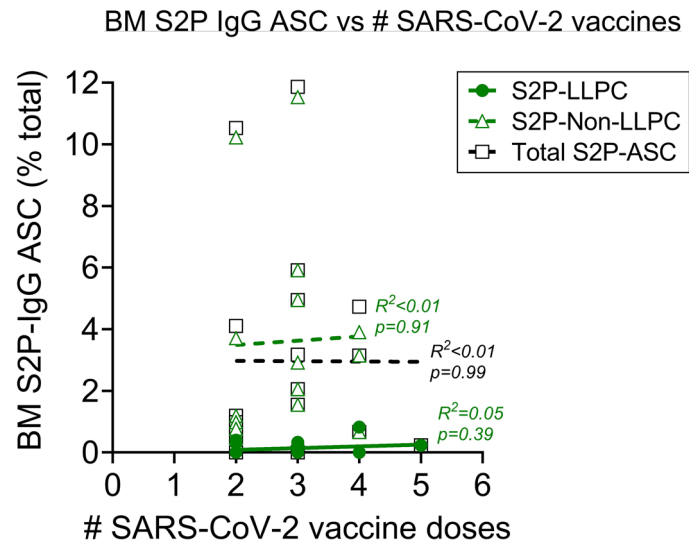
Extended Data Fig. 6 | No correlation between S2P IgG BM ASC responses and the number of SARS-CoV-2 vaccine doses. BM S2P IgG ASC responses in all examined subjects stratified by the number of SARS-CoV-2 vaccine doses (prior to BM aspiration). Data were generated from 17, 15, and 19 different SARS-CoV-2 vaccinated subjects for BM LLPC, Non-LLPC, and total ASC, respectively. The exact p values for S2P LLPC, Non-LLPC, and total ASC are 0.3929, 0.9110, and 0.9912, respectively. Subjects yielding sufficient ASC for LLPC and Non-LLPC subsets included.
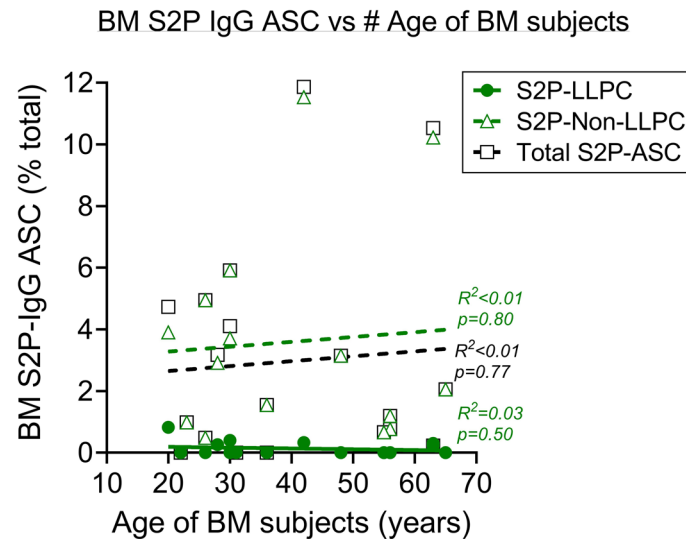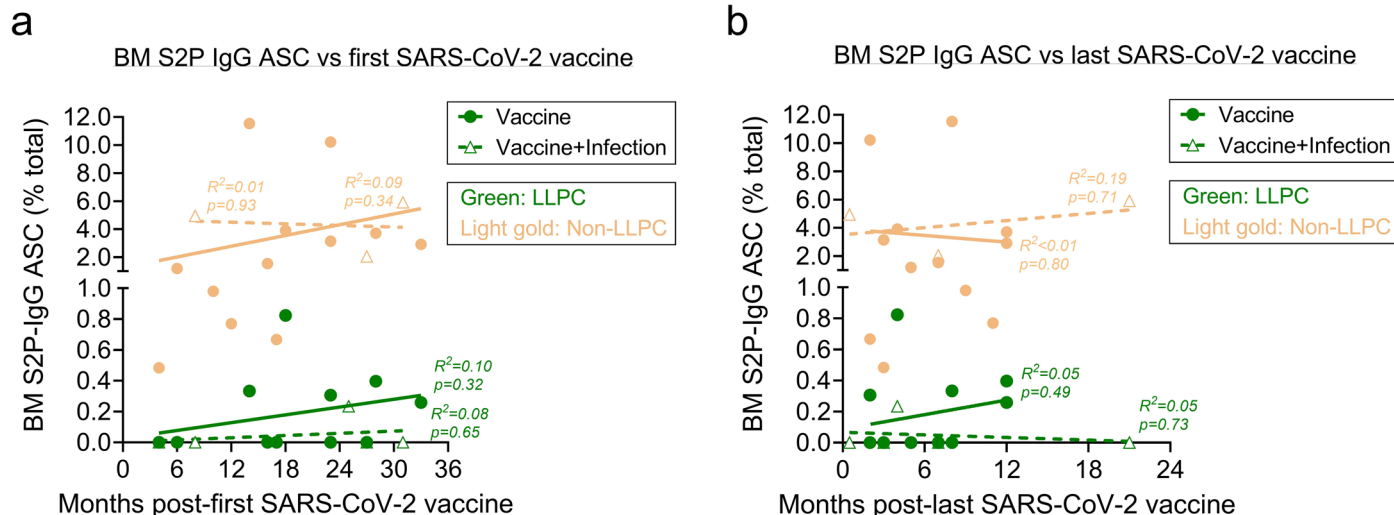
Extended Data Fig. 7 | No correlation between S2P IgG BM ASC responses and age of the subjects. BM S2P IgG ASC responses in all examined subjects stratified by age of the subjects at the time of BM collection. Data were generated from 17, 15, and 19 different SARS-CoV-2 vaccinated subjects for BM LLPC, Non-LLPC, and total ASC, respectively. The exact p values for S2P LLPC, Non-LLPC, and total ASC are 0.4950, 0.7976, and 0.7699, respectively. Subjects yielding sufficient ASC for LLPC and Non-LLPC subsets included.

a

BM S2P IgG ASC vs first SARS-CoV-2 vaccine

b

BM S2P IgG ASC vs last SARS-CoV-2 vaccine

Extended Data Fig. 8 | No correlation between S2P IgG BM ASC responses and the time windows of the SARS-CoV-2 vaccine in both vaccinees and infected vaccinees (Vaccine+Infection). BM S2P IgG SC responses in vaccinated versus hybrid subjects stratified by time since (**a**) the first or (**b**) the most recent (prior to BM aspiration) SARS-CoV-2 vaccine. The exposure time for infection in the hybrid subjects not shown. For BM LLPC, data were generated from 12 and 5 different subjects of Vaccine and of Vaccine+Infection, respectively. For

BM Non-LLPC, data were generated from 12 and 3 different subjects of Vaccine and of Vaccine+Infection, respectively. The exact p values for Vaccine/LLPC, Vaccine+Infection/LLPC, Vaccine/Non-LLPC, and Vaccine+Infection/Non-LLPC are 0.3192, 0.6529, 0.3446, and 0.9254, respectively (**a**); and 0.4933, 0.7301, 0.8004, and 0.7128, respectively (**b**). Subjects yielding sufficient ASC for LLPC and Non-LLPC subsets included.

a

b
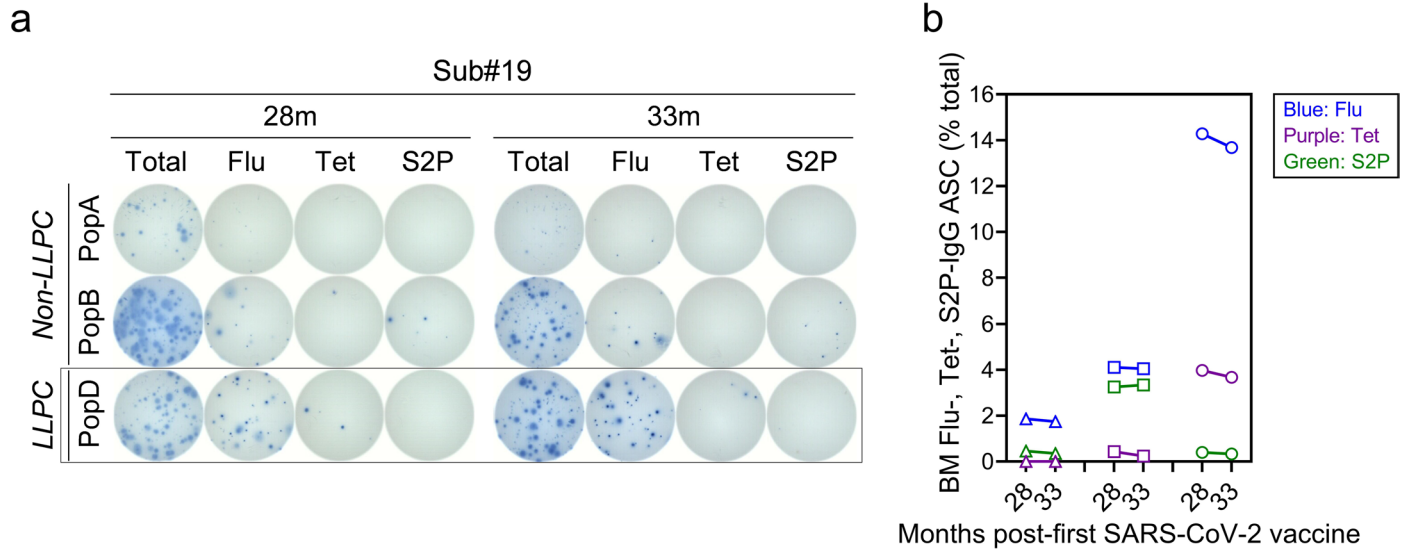
Extended Data Fig. 9 | Kinetics of vaccine-specific IgG ASC responses in the subject who donated two sequential BM aspirates (at 28 and 33 months after the first SARS-CoV-2 vaccine). (**a**) ELISpot scanned images. The numbers of input ASC incubated were ~3.04 K, ~1.27 K, and ~0.88 K (28 m, total), ~15.20 K, ~7.61 K, and ~2.65 K (28 m, vaccine-specific); and ~1.56 K, ~1.02 K, and ~0.75 K (33 m, total), and ~18.67 K, ~7.12 K, and ~2.98 K (33 m, vaccine-specific), for PopA, PopB, and PopD, respectively. (**b**) Vaccine-specific IgG ASC response kinetics. ~: counts provided by the sorters; K: 1,000; LLPC: long-lived plasma cell (box); Flu: influenza; Tet: tetanus; m: month. For details of the subject, see Table 1.
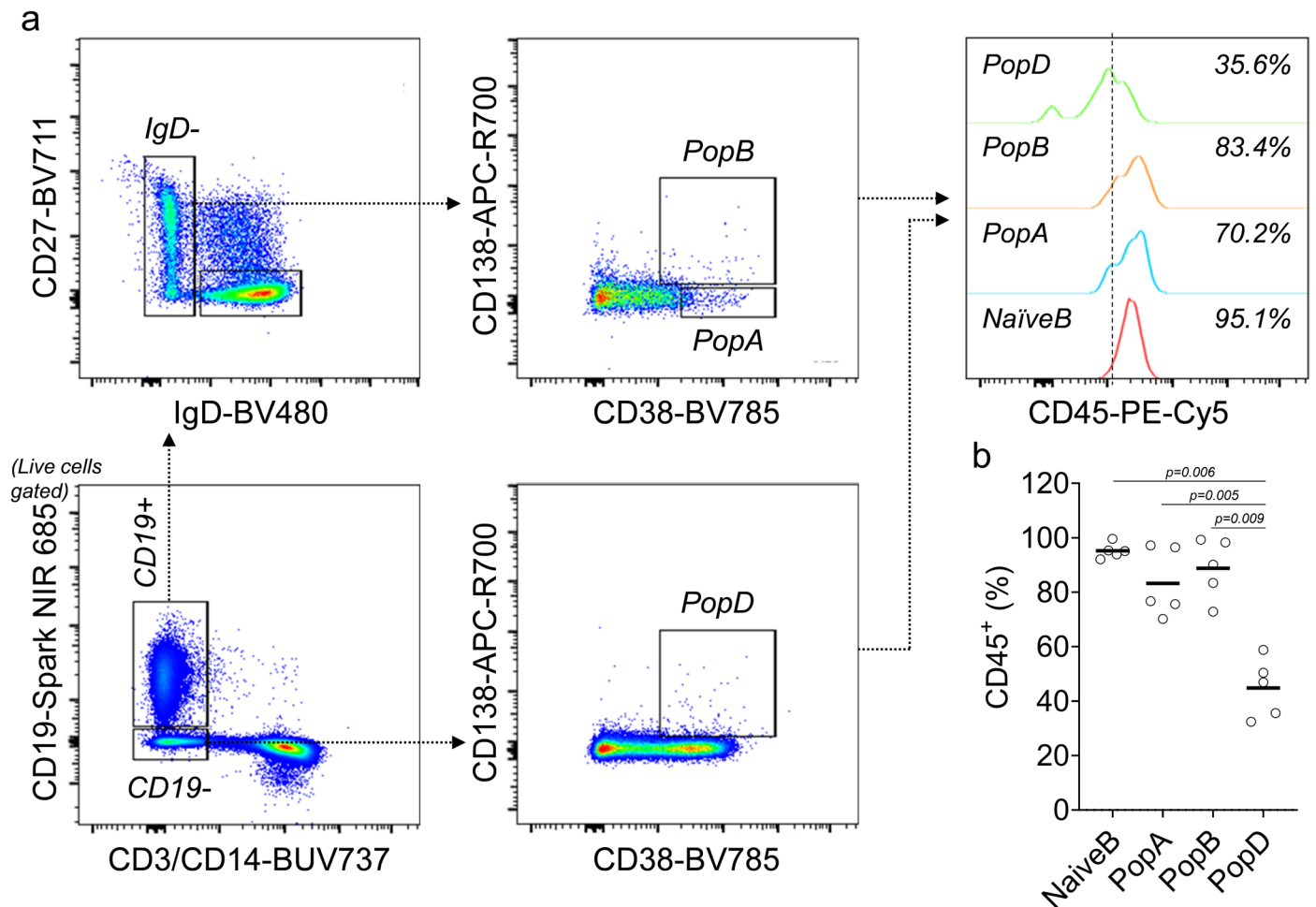
Extended Data Fig. 10 | Downregulation of CD45 in LLPC (PopD).
(**a**) Representative FACS gating strategy and CD45 staining for BM ASC subsets. For details on BM ASC gating, see Fig. 1b. For the antibody panels, see Methods. (**b**) CD45 staining is downregulated in PopD. Each circle represents an individual healthy BM donor. Data were generated from five different healthy BM donors.

Statistic comparisons between any two CD45+ subsets were assessed using Student's t-test (two-tailed unpaired t-test) in Excel (Microsoft) and differences were considered significant at p values less than 0.05. Shown are p values from comparisons with PopD; for p values from comparisons between other subsets, see Supplementary Table 5.

Corresponding author(s): F. Eun-Hyung Lee, MD

Last updated by author(s): Aug 6, 2024

Reporting Summary

Nature Portfolio wishes to improve the reproducibility of the work that we publish. This form provides structure for consistency and transparency in reporting. For further information on Nature Portfolio policies, see our Editorial Policies and the Editorial Policy Checklist.

Statistics

For all statistical analyses, confirm that the following items are present in the figure legend, table legend, main text, or Methods section.

n/a	Confirmed	
☐	☒	The exact sample size (*n*) for each experimental group/condition, given as a discrete number and unit of measurement
☐	☒	A statement on whether measurements were taken from distinct samples or whether the same sample was measured repeatedly
☐	☒	The statistical test(s) used AND whether they are one- or two-sided *Only common tests should be described solely by name; describe more complex techniques in the Methods section.*
☒	☐	A description of all covariates tested
☐	☒	A description of any assumptions or corrections, such as tests of normality and adjustment for multiple comparisons
☐	☒	A full description of the statistical parameters including central tendency (e.g. means) or other basic estimates (e.g. regression coefficient) AND variation (e.g. standard deviation) or associated estimates of uncertainty (e.g. confidence intervals)
☐	☒	For null hypothesis testing, the test statistic (e.g. *F*, *t*, *r*) with confidence intervals, effect sizes, degrees of freedom and *P* value noted *Give P values as exact values whenever suitable.*
☒	☐	For Bayesian analysis, information on the choice of priors and Markov chain Monte Carlo settings
☒	☐	For hierarchical and complex designs, identification of the appropriate level for tests and full reporting of outcomes
☒	☐	Estimates of effect sizes (e.g. Cohen's *d*, Pearson's *r*), indicating how they were calculated

Our web collection on statistics for biologists contains articles on many of the points above.

Software and code

Policy information about availability of computer code

Data collection	Donor data was collected using RedCAP data capture software. ELISpot data was collected using the Cellular Technology Limited system (CTL; Shaker Heights, OH, USA), which run ImmunoSpot 5.0.9.21 software. Multiplex bead binding assay data (including antigen specific data) was analyzed using a Luminex FLEXMAP 3D®instrument (Luminex; Austin, TX, USA), which run xPonent 4.3 software. Flow cytometry data was collected on a Cytek Aurora Spectral Flow Cytometer using Cytek SpectroFlo software (v3.0; Cytek Biosciences) and analyzed with the FlowJo software (v10.8.1; FlowJo, LLC).
Data analysis	Statistical analyses were assessed using Student's t-test (two-tailed unpaired t-test) or one-way ANOVA performed with GraphPad Prism (v8.4.2; GraphPad Software; Boston, MA, USA).

For manuscripts utilizing custom algorithms or software that are central to the research but not yet described in published literature, software must be made available to editors and reviewers. We strongly encourage code deposition in a community repository (e.g. GitHub). See the Nature Portfolio guidelines for submitting code & software for further information.

Data

Policy information about availability of data

All manuscripts must include a data availability statement. This statement should provide the following information, where applicable:
- Accession codes, unique identifiers, or web links for publicly available datasets
- A description of any restrictions on data availability
- For clinical datasets or third party data, please ensure that the statement adheres to our policy

> There is no restriction on experimental data availability from this study. All the datasets generated during and/or analysed during the current study are available from the corresponding author. There is no data with mandated deposition is presented in this study. Also, there is no bulk sequencing data nor single cell VDJ sequencing data were presented in this study.

Human research participants

Policy information about studies involving human research participants and Sex and Gender in Research.

Reporting on sex and gender	Sex & gender information was collected for subject characteristics purpose only but was not relevant to this study. Sex- & gender-based analyses were not performed in this study.
Population characteristics	Population characteristics are fully described in Table 1 of the manuscript.
Recruitment	Written informed consent was obtained from all participants or, if they were unable to provide informed consent, obtained from designated healthcare surrogates. Healthy subjects were recruited using promotional materials approved by the Emory University Institutional Review Board. There were no potential self-selection bias or other biases that may be present or likely to impact results.
Ethics oversight	Written informed consent was obatined from all subjects. All research was approved by the Emory University Institutional Review Board (Emory IRB numbers IRB00066294 and IRB00057983) and was performed in accordance with all relevant guidelines and regulations.

Note that full information on the approval of the study protocol must also be provided in the manuscript.

Field-specific reporting

Please select the one below that is the best fit for your research. If you are not sure, read the appropriate sections before making your selection.

☒ Life sciences   ☐ Behavioural & social sciences   ☐ Ecological, evolutionary & environmental sciences

For a reference copy of the document with all sections, see nature.com/documents/nr-reporting-summary-flat.pdf

Life sciences study design

All studies must disclose on these points even when the disclosure is negative.

Sample size	No statistical method was used to pre-determine sample size and sample size was pre-selected. Samples were collected over three years to be confident the results were statistically significant to distinguish different biological antigen-specific BM subsets.
Data exclusions	To make sure the quantity of antibody secreting cells (ASC) was sufficient for antigen specificity assays, all subjects with <3,000 sorted ASC in each of the three bone marrow ASC populations was excluded from the study. No other criteria were used to exclude any subjects from the analysis.
Replication	Replication could not be done on this cohort due to limitations in both donor and sample (bone marrow) availability and cost. However, donor samples were collected, processed, and analyzed on different days and by a small group of certain different personnel. The nature of this study does not lend itself to simple replication; however, all analysis presented maintained consistency over time and within technical replicates.
Randomization	Given the exploratory nature of this study, no randomization was performed.
Blinding	Blinding was not relevant to this study. We recruited adult subjects who are healthy as defined by a health survey with no history of autoimmune, renal, liver, cardiopulmonary, and vascular disease. Patients with history of malignancy, transplant, HIV, hepatitis C, or those on immunosuppressive therapies are also excluded. The investigators were not blinded to allocation during experiments and outcome assessment.

Reporting for specific materials, systems and methods

We require information from authors about some types of materials, experimental systems and methods used in many studies. Here, indicate whether each material, system or method listed is relevant to your study. If you are not sure if a list item applies to your research, read the appropriate section before selecting a response.

Materials & experimental systems

n/a	Involved in the study
☐	☒ Antibodies
☒	☐ Eukaryotic cell lines
☒	☐ Palaeontology and archaeology
☒	☐ Animals and other organisms
☒	☐ Clinical data
☒	☐ Dual use research of concern

Methods

n/a	Involved in the study
☒	☐ ChIP-seq
☐	☒ Flow cytometry
☒	☐ MRI-based neuroimaging

Antibodies

Antibodies used

For the antibody-secreting cell sorting panels, cellular enriched fractions from blood or bone marrow aspirates were stained with the following anti-human antibodies: IgD–FITC (Cat. #555778; BD Biosciences) at 1:5 dilution or IgD-Brilliant Violet 480 (Cat. #566138; BD Biosciences) at 1:5 dilution, CD3-BV711 (Cat. #317328; BioLegend) at 1:20 dilution or CD3-BUV737 (Cat. #612750; BD Biosciences) at 1:20 dilution, CD14-BV711 (Cat. #301838; BioLegend) at 1:20 dilution or CD14-BUV737 (Cat. #612763; BD Biosciences) at 1:20 dilution, CD19-PE-Cy7 (Cat. #560911; BD Biosciences) at 1:5 dilution or CD19-Spark NIR 685 (Cat. #302270; BioLegend) at 1:5 dilution, CD38-V450 (Cat. #561378; BD Bioscience) at 1:20 dilution or CD38-Brilliant Violet 785 (Cat. #303530; BioLegend) at 1:20 dilution, CD138-APC (Cat. #130-117-395; Miltenyi Biotech) at 1:20 dilution or CD138-APC-R700 (Cat. #566050; BD Biosciences) at 1:20 dilution, CD27-APC-e780 (Cat. #5016160; eBiosciences) at 1:20 dilution or CD27-Brilliant Violet 711 (Cat. #356430; BioLegend) at 1:20 dilution, and LiveDead (Cat. #L34966; Invitrogen) at 1:600 dilution or Zombie NIR Fixable Viability Kit (Cat. #423106; BioLegend) at 1:500 dilution.

For the panel for CD45 BM ASC flow cytometry, bone marrow mononuclear cells were stained with the following anti-human antibodies: IgD-Brilliant Violet 480 (Cat. #566138; BD Biosciences) at 1:160 dilution, CD3-BUV737 (Cat. #612750; BD Biosciences) at 1:160 dilution, CD14-BUV737 (Cat. #612763; BD Biosciences) at 1:160 dilution, CD19-Spark NIR 685 (Cat. #302270; BioLegend) at 1:160 dilution, CD38-Brilliant Violet 785 (Cat. #303530; BioLegend) at 1:160 dilution, CD138-APC-R700 (Cat. #566050; BD Biosciences) at 1:320 dilution, CD27-Brilliant Violet 711 (Cat. #356430; BioLegend) at 1:40 dilution, and CD45-PE-Cy5 (Cat. #304009; BioLegend) at 1:40 dilution.

For relative quantitation of antigen-specific antibody titers, standard curves were generated using monoclonal antibody (mAb) standards of anti-tetanus toxin mAb (clone #TetE3; The Native Antigen Company; Cat. #MAB12239-100) at 1:1,000-1:1,000,000,000 dilutions (10-fold serial dilution) and SARS-CoV-2-reactive (spike RBD) mAb (Abeomics; Cat. #ABMX-002) at 1:1,000-1:1,000,000,000 dilutions (10-fold serial dilution). For determining the concentrations of total IgG, purified human IgG (ChromePure human IgG, JacksonImmuno Research Laboratories; Cat. #009-000-003) was used as a standard.

Validation

All antibodies have been validated by the manufacturer for use in targeting human proteins as indicated above. Furthermore, all antibodies were also validated experimentally by our own research groups who used them for over a decade.

IgD–FITC (Cat. #555778; BD Biosciences)
The antibody has been validated by the manufacturer for FACS use on human samples. Its validation statement: "This antibody is routinely tested by flow cytometric analysis. Other applications were tested at BD Biosciences Pharmingen during antibody development only or reported in the literature."
Application references: The Journal of Clinical Investigation on 1 October 2019 by Conde, C. D., Petronczki, Ö. Y., et al.; Immunity & Ageing: I & A on 17 July 2023 by Frasca, D., Romero, M., et al.; Frontiers in Immunology on 13 March 2021 by Frasca, D., Diaz, A., et al.; International Journal of Molecular Sciences on 12 February 2021 by Frasca, D., Romero, M., et al.; Oncoimmunology on 2 February 2021 by de Jonge, K., Tillé, L., et al.
Our own validation: see our published papers below.

CD3-BV711 (Cat. #317328; BioLegend)
The antibody has been validated by the manufacturer for FACS use on human samples. Its validation statement: "this antibody is quality control tested by immunofluorescent staining with flow cytometric analysis. For flow cytometric staining, the suggested use of this reagent is 5 μl per million cells in 100 μl staining volume or 5 μl per 100 μl of whole blood."
Application references: Schlossman S, et al. Eds. 1995. Leucocyte Typing V. Oxford University Press. New York; Knapp W. 1989. Leucocyte Typing IV. Oxford University Press New York; Barclay N, et al. 1997. The Leucocyte Antigen Facts Book. Academic Press Inc. San Diego; Li B, et al. 2005. Immunology 116:487.
Jeong HY, et al. 2008. J. Leuckocyte Biol. 83:755; Alter G, et al. 2008. J. Virol. 82:9668; Manevich-Mendelson E, et al. 2009. Blood 114:2344; Pinto JP, et al. 2010. Immunology. 130:217; Biggs MJ, et al. 2011. J. R. Soc. Interface. 8:1462.
Our own validation: see our published papers below.

CD14-BV711 (Cat. #301838; BioLegend)
The antibody has been validated by the manufacturer for FACS use on human samples. Its validation statement: "this antibody is quality control tested by immunofluorescent staining with flow cytometric analysis. For flow cytometric staining, the suggested use of

this reagent is 5 μl per million cells in 100 μl staining volume or 5 μl per 100 μl of whole blood."
Application references: McMichael A, et al. 1987. Leucocyte Typing III. Oxford University Press. New York;
Power CP, et al. 2004. J. Immunol. 173:5229; Williams KC, et al. 2001. J. Exp. Med. 193:905; Iwamoto S, et al. 2007. J. Immunol. 179:1449; Santer DM, et al. 2010. J. Immunol. 485:4739; Yoshino N, et al. 2000. Exp. Anim. (Tokyo) 49:97; Zizzo G, et al. 2012. J. Immunol. 189:3508.
Our own validation: see our published papers below.

CD19-PE-Cy7 (Cat. #560911; BD Biosciences)
The antibody has been validated by the manufacturer for FACS use on human samples. Its validation statement: "Flow cytometry (Routinely Tested)."
Application references: Bradbury LE et al. J Immunol. 1993; 151(6):2915-2927; Favaloro EJ et al. Thromb
Haemost. 1989; 61(2):217-224; Nadler LM et al. J Immunol. 1983; 131(1):244-250. Roederer M et al. Cytometry. 1996; 24(3):191-197. Uckun FM et al. Blood. 1989; 73(4):1000-1015.
Our own validation: see our published papers below.

CD38-V450 (Cat. #561378; BD Bioscience)
The antibody has been validated by the manufacturer for FACS use on human samples. Its validation statement: "The antibody is conjugated to BD Horizon™ V450, which has been developed for use in multicolor flow cytometry experiments" & "Flow cytometry (Routinely Tested)."
Application references: McMichael AJ et al. ed. Leukocyte Typing III: White Cell Differentiation Antigens. New York: Oxford University Press; 1987; Schlossman SF et al. ed. Leukocyte Typing V: White Cell Differentiation Antigens. New York: Oxford University Press; 1995.
Our own validation: see our published papers below.

CD138-APC (Cat. #130-117-395; Miltenyi Biotech)
The antibody has been validated by the manufacturer for FACS use on human samples. Its validation statement: "... stained with CD138 antibodies and analyzed by flow cytometry."
Application references: Suan et al. Immunity. 2017 Dec 19;47(6):1142-1153.e4; Miggitsch et al. EBioMedicine. 2019 Aug:46:387-398; Hartog et al. Eur J Immunol. 2018 Feb;48(2):283-292
Our own validation: see our published papers below.

CD27-APC-e780 (Cat. #5016160; eBiosciences)
The antibody has been validated by the manufacturer for FACS use on human samples. Its validation statement: "This antibody has been reported for use in flow cytometric analysis." & "This antibody has been pre-titrated and tested by flow cytometric analysis of normal human peripheral blood cells. This can be used at 5 μL (0.25 μg) per test. A test is defined as the amount (μg) of antibody that will stain a cell sample in a final volume of 100 μL."
Our own validation: see our published papers below.

CD45-PE-Cy5 (Cat. #304009; BioLegend)
The antibody has been validated by the manufacturer for FACS use on human samples. Its validation statement: "this antibody is quality control tested by immunofluorescent staining with flow cytometric analysis. For flow cytometric staining, the suggested use of this reagent is 5 μl per million cells in 100 μl staining volume or 5 μl per 100 μl of whole blood."
Application references: Knapp W, et al. 1989. Leucocyte Typing IV. Oxford University Press. New York.
Kishihara K, et al. 1993. Cell 74:143; Yamada T, et al. 2002. J. Biol. Chem. 277:28830; Nagano M, et al. 2007. Blood 110:151; Jiang Q, et al. 2008. Blood 112:2858; Morozov A, et al. 2010. Clin Cancer Res. 16:5630; Yoshino N, et al. 2000. Exp. Anim. (Tokyo) 49:97; Oeztuerk-Winder F, et al. 2012. EMBO J. 31:3431; & Lee J, et al. 2015. J Exp Med. 212:385.

Citations in our own published papers:
Halliley, J. L. et al. Long-Lived Plasma Cells Are Contained within the CD19(-)CD38(hi)CD138(+) Subset in Human Bone Marrow. Immunity 43, 132-145, doi:10.1016/j.immuni.2015.06.016 (2015).

Nguyen, D. C. et al. Factors of the bone marrow microniche that support human plasma cell survival and immunoglobulin secretion. Nat Commun 9, 3698, doi:10.1038/s41467-018-05853-7 (2018).

Nguyen, D. C. et al. Extracellular vesicles from bone marrow-derived mesenchymal stromal cells support ex vivo survival of human antibody secreting cells. J Extracell Vesicles. 2018 Apr 26;7(1):1463778.

Garimalla S., Nguyen D. C. et al. Differential transcriptome and development of human peripheral plasma cell subsets. JCI Insight. 2019 May 2;4(9):e126732.

Joyner, C. J., Ley A., Nguyen D. C. et al. Generation of human long-lived plasma cells by developmentally regulated epigenetic imprinting. Life Sci Alliance 5, doi:10.26508/lsa.202101285 (2022).

Duan, M. et al. Understanding heterogeneity of human bone marrow plasma cell maturation and survival pathways by single-cell analyses. Cell Rep 42, 112682, doi:10.1016/j.celrep.2023.112682 (2023).

Nguyen, D. C. et al. Majority of human circulating IgG plasmablasts stop blasting in a cell-free pro-survival culture. Sci Rep 14, 3616, doi:10.1038/s41598-024-53977-2 (2024).

Flow Cytometry

Plots

Confirm that:

☒ The axis labels state the marker and fluorochrome used (e.g. CD4-FITC).

☒ The axis scales are clearly visible. Include numbers along axes only for bottom left plot of group (a 'group' is an analysis of identical markers).

☒ All plots are contour plots with outliers or pseudocolor plots.

☒ A numerical value for number of cells or percentage (with statistics) is provided.

Methodology

Sample preparation	Peripheral blood samples & bone marrow aspirates were collected in heparin sodium tubes & processed within 1-2 hours of collection. Peripheral blood and bone marrow mononuclear cells (MNC) were isolated by density gradient centrifugation at 1000 x g for 10 minutes. MNC were subsequently enriched by either a commercial human Pan-B cell enrichment kit (that removes cells expressing CD2, CD3, CD14, CD16, CD36, CD42b, CD56, CD66b, CD123, and glycophorin A) (StemCell Technologies) or a custom-designed negative selection cell isolation kit (that removes cells expressing CD3, CD14, CD66b, and glycophorin A) (StemCell Technologies) in prior to being stained with the following above-mentioned antibody panels. Post-sort ASC off-sorter were cultured in MSC secretome (ASC survival medium) at 37°C overnight. Cultured cells were then collected for ELISpot assaying for IgG & IgA secreting ASC & the culture supernatants were collected for multiplex bead binding assays for detection/quantification of secreted IgG.
Instrument	For CD45 flow cytometric analysis, stained bone marrow mononuclear cells were analyzed on a Cytek's Aurora Spectral Flow Cytometer using Cytek SpectroFlo software.
Software	Cells were analyzed on a Cytek Aurora flow cytometer using Cytek SpectroFlo software. Up to 3 x 106 cells were analyzed using FlowJo vl0 (Treestar) software.
Cell population abundance	The yields for bone marrow ASC subsets post-sort vary greatly among different subsets & from sample to sample. Sorted ASC populations were generally 93-99% pure except for PopA (whose purity was usually ~60-75%) when checked upon the sorts being finished.
Gating strategy	Gating strategy is provided in Figure 1b (bone marrow samples) & Supplemental Figure S1 (blood samples).

Briefly, bone marrow MNC were first gated for lymphocytes, singlets, and viable cells (based on their FSC/SSC and Live/Death properties). CD3 and CD14 were then used as dump markers to capture CD19+ and CD19- B cell populations. Subsequent sub-gating from CD19+ population on the IgD- fraction (versus CD27) and using CD138 versus CD38 allow for breaking down bone marrow ASC populations into 3 subsets of interest: PopA (CD19+CD38hiCD138-), PopB (CD19+CD38hiCD138+), and PopD (LLPC; CD19-CD38hiCD138-).

For blood samples, peripheral blood mononuclear cells were also first gated for lymphocytes, singlets, and viable cells (based on their FSC/SSC and Live/Death properties). CD3 and CD14 were then used as dump markers to capture CD19+ and CD19- B cell populations. Subsequent sub-gating using CD38 versus CD27 on the IgD- fraction (of CD19+ population) allows for sorting for blood ASC (CD27hiCD38hi). |

☒ Tick this box to confirm that a figure exemplifying the gating strategy is provided in the Supplementary Information.